

Estimation of conditional average treatment effects on distributed data: A privacy-preserving approach

Yuji Kawamata *

Center for Artificial Intelligence Research, University of Tsukuba, Japan

Ryoki Motai

Graduate School of Science and Technology, University of Tsukuba, Japan

Yukihiko Okada

Center for Artificial Intelligence Research, University of Tsukuba, Japan

Akira Imakura

Center for Artificial Intelligence Research, University of Tsukuba, Japan
and

Tetsuya Sakurai

Center for Artificial Intelligence Research, University of Tsukuba, Japan

May 28, 2024

Abstract

Estimation of conditional average treatment effects (CATEs) is an important topic in sciences. CATEs can be estimated with high accuracy if distributed data across multiple parties can be centralized. However, it is difficult to aggregate such data owing to privacy concerns. To address this issue, we proposed data collaboration double machine learning, a method that can estimate CATE models with privacy preservation of distributed data, and evaluated the method through simulations. Our contributions are summarized in the following three points. First, our method enables estimation and testing of semi-parametric CATE models without iterative communication on distributed data. Semi-parametric CATE models enable estimation and testing that is more robust to model mis-specification than parametric models. Second, our method enables collaborative estimation between multiple time points and different parties. Third, our method performed equally or better than other methods in simulations using synthetic, semi-synthetic and real-world datasets.

Keywords: Data collaboration framework; Double machine learning; Statistical causal inference;

*The authors gratefully acknowledge the *New Energy and Industrial Technology Development Organization (NEDO)* (No. JPNP18010), *Japan Science and Technology Agency (JST)* (No. JPMJPF2017), *Japan Society for the Promotion of Science (JSPS)*, and *Grants-in-Aid for Scientific Research* (Nos. JP19KK0255, JP21H03451, JP23K22166, JP22K19767). Email: yjkawamata@gmail.com

1 Introduction

The Neyman–Rubin model (Imbens and Rubin, 2015) or potential outcomes framework is one of the main causal inference methods for estimating average treatment (intervention) effects and has been developed and applied in many studies since its establishment by Rubin. In recent years, there have been innovations that enable the estimation of individual or conditional average treatment effects (CATEs) by adapting not only statistical but also machine learning methods. (e.g., Künzel et al. (2019); Athey et al. (2019)) Most methods for estimating CATEs assume that the data can be centralized in one place. However, if the distributed data contains confidential or private information, it is difficult to centralized them in one place.

Conversely, in the field of machine learning, a privacy-preserving analysis method called federated learning has been developed in recent years. (Konečný et al., 2016; McMahan et al., 2017; Wu et al., 2023) Data collaboration (DC) analysis (Imakura and Sakurai, 2020; Bogdanova et al., 2020; Imakura et al., 2021, 2023), one of federated learning systems, is a method that allows collaborative analysis with privacy preservation by sharing dimensionality-reduced intermediate representations instead of raw data. DC analysis was originally proposed to construct regression and classification models from distributed data. Recently, Kawamata et al. (2024) proposed data collaboration quasi-experiment (DC-QE), that extends DC analysis to allow estimation of average treatment effect (ATE). In this paper, we propose data collaboration double machine learning (DC-DML) as a method to estimate CATEs while preserving the privacy of distributed data by incorporating double machine learning (DML) (Chernozhukov et al., 2018), a machine learning-based treatment effect estimation method, into DC-QE. Moreover, through numerical simulations, we evaluate the performance of our method compared to existing methods.

This paper relates partially linear models, one of the semi-parametric models. Since

Engle et al. (1986), partially linear models have been used in empirical studies where assuming a linear model between the covariates and the outcome is not appropriate, i.e., to avoid model mis-specification owing to linear assumptions. A significant advance about partially linear models in recent years is DML (Chernozhukov et al., 2018), which brought an least square estimator that can adapt common machine learning models. Various causal inference methods have been developed by developing DML (Fan et al., 2022; Bia et al., 2023). In this paper, we develop DML into a method that enables CATE estimation through distributed data with privacy preservation.

The effects of policy interventions by governments or medical treatments by hospitals are likely to differ across people. It is possible to improve the overall performance of the treatment if one knows which individuals should be treated. For example, by concentrating scholarship support on those whose future income increases will be higher owing to the treatment, the limited budget can be used more efficiently. In addition, by concentrating medication on those who are more likely to improved or have fewer side effects from the treatment, medication can be more effective and safer to use. One approach to estimating CATEs for these situations with a high accuracy is to centralize data from many parties, but this is difficult owing to privacy concerns. Our method enables to estimate CATEs with high accuracy while maintaining the privacy of distributed data across many parties.

Our contributions are summarized in the following three points. First, our method enables estimation and testing of semi-parametric CATE models without iterative communication on distributed data. Semi-parametric (or non-parametric) CATE models enable estimation and testing that is more robust to model mis-specification than parametric models. However, to our knowledge, no communication-efficient method has been proposed for estimating and testing semi-parametric (or non-parametric) CATE models on distributed data. Second, our method enables collaborative estimation between different parties as well as multiple time points because the dimensionality-reduced intermediate representa-

tions can be accumulated. Third, our method performed as well or better than other methods in evaluation simulations using synthetic, semi-synthetic and real-world datasets.

The remainder of this paper is organized as follows. In Section 2, we present related works on causal inference and machine learning. We describe the basics of causal inference and distributed data in Section 3. We describe our method in Section 4. In Section 5, we report the numerical simulations and discuss the results. Finally, we conclude in Section 6.

2 Related works

The field of treatment effect estimation has advanced significantly in recent years through the incorporation of machine learning methods as well as statistics. However, studies that take into account privacy preservation, which is our aim, are limited. Here, we briefly review existing methods.

DML is an innovative method proposed by Chernozhukov et al. (2018) that allows estimation of ATE using any machine learning methods. DML is a semi-parametric method that uses machine learning to estimate nuisance parameters for estimating target parameters. More specifically, DML first estimates nuisance parameters using machine learning, and then estimates the target parameters using the estimated nuisance parameters. DML resolves influences of regularization bias and over-fitting on estimates of target parameters through Neyman–orthogonal scores and cross-fitting, respectively. As shown in Section 3, DML can be extended easily to allow estimation of CATE. DML is a useful method for estimating treatment effects, but using centralized data. To achieve our goal, we need to develop DML to address distributed data. In Section 3, we describe DML in detail.

As representative methods that utilize machine learning for CATE estimation, generalized random forest (GRF) (Athey et al., 2019) and X-Learner (Künzel et al., 2019) have been proposed, but these methods cannot be applied to distributed data. GRF is a

non-parametric method for estimating treatment effects by solving local moment equations using random forests. GRF first constructs a random forest, then calculates weights for each sample from the random forest, and finally derives the treatment effect by solving a moment equations using the calculated weights. X-Learner is a non-parametric method that can estimate treatment effects from any machine learning model. X-Learner uses propensity scores (Rosenbaum and Rubin, 1983) to resolve performance degradation that occurs when controlled or treated group is much larger than the other group.

Conversely, Secure regression (SR) (Karr et al., 2005) and FedCI (Vo et al., 2022) are methods that can estimate CATEs from distributed data. SR is a parametric method for estimating linear regression models. In SR, statistics necessary to compute least squares estimates are calculated in each local party, and these statistics are shared. SR is communication-efficient because it enables estimation of a linear model by sharing statistics only once. However, in SR, bias owing to mis-specification can occur if the assumptions of the linear model are incorrect. FedCI is a non-parametric method that constructs a potential outcome model based on Gaussian processes through federated learning approach. In FedCI, the communication between the clients and the server is iterated: each client sends the model gradient calculated from its local data to the server, then the server averages the aggregated gradients, updates its own model parameters, and returns those parameters to the clients. In the case where local data is stored in a location isolated from the Internet or synchronization of communications is not possible, FedCI is difficult to execute.

While the purpose of our method is to estimate CATEs, ifedtree (Tan et al., 2022), Federated MLE, IPW and AIPW (Xiong et al., 2023), and DC-QE (Kawamata et al., 2024) are methods that have been proposed for different estimation targets. Those methods can address distributed data. ifedtree is a tree-based model averaging approach to improve the CATE estimation at a specific party by sharing models derived from other parties instead of raw data. Our method aims to estimate CATEs on aggregated whole data, rather than

Methods	Can it deal with distributed data?	Assumptions of CATE model	Does it need iterative communication?
DML (Chernozhukov et al., 2018)	No	Semi-parametric	-
GRF (Athey et al., 2019)	No	Non-parametric	-
X-Learner (Künzel et al., 2019)	No	Non-parametric	-
SR (Karr et al., 2005)	Yes	Parametric	No
FedCI (Vo et al., 2022)	Yes	Non-parametric	Yes
DC-DML (our method)	Yes	Semi-parametric	No

Table 1: Existing and our methods.

on specific party data. Federated MLE, IPW and AIPW are a parametric methods that aggregates individually estimated gradients for estimating propensity scores and treatment effects. Federated MLE, IPW and AIPW estimate the ATE not conditioned on covariates.

DC-QE is a semi-parametric method for estimating ATE and ATT based on a DC analysis framework. DC-QE first construct collaborative representations based on dimensionality-reduced intermediate representations collected from all parties instead of raw data, second estimates propensity scores, finally estimates ATE or ATT using the estimated propensity scores (see supplemental material A for details). Our method extends DC-QE to address DML for CATE estimation.

Table 1 summarizes five of those described in this section that are particularly relevant to our method. In Section 4, we propose a method for estimating CATEs in a semi-parametric model while preserving privacy of distributed data. Although DML, GRF and X-Learner are methods for centralized data, our method address distributed data. Moreover, our method is more robust than SR for model misspecification and more communication-efficient than FedCI.

3 DML with the linear CATE model

In this section, we describe the DML method with the linear CATE model. Under the Neyman–Rubin causal model, let variables for subject i as $y_i(0)$, $y_i(1)$, z_i and \mathbf{x}_i , where $\mathbf{x}_i = (x_i^1, \dots, x_i^m)^\top \in \mathbb{R}^m$ is the m -dimensional covariates vector, $z_i \in \{0, 1\}$ is the treatment, $y_i(1)$ is the outcome that subject i would have if they were treated ($z_i = 1$), and $y_i(0)$ is that if not (controlled; $z_i = 0$). Moreover, we denote $y_i = y_i(z_i)$. With this definition, the CATE is defined as

$$\tau(\mathbf{x}_i) = \mathbb{E}[y_i(1) - y_i(0)|\mathbf{x}_i].$$

In DML, we make the following structural equation assumptions on the data generating process as

$$y_i = \theta(\mathbf{x}_i) \cdot z_i + u(\mathbf{x}_i) + \varepsilon_i,$$

$$z_i = h(\mathbf{x}_i) + \eta_i.$$

θ is the function that represents the effect of the treatment conditional on the covariate \mathbf{x}_i . The covariates \mathbf{x}_i affect the treatment z_i via the function h and the outcome via the function u , where h and u are defined as functions belong to convex subsets \mathbb{H} and \mathbb{U} with some normed vector space. ε_i and η_i are disturbances such that $\mathbb{E}[\eta_i|\mathbf{x}_i] = 0$, $\mathbb{E}[\varepsilon_i|\mathbf{x}_i] = 0$ and $\mathbb{E}[\eta_i\varepsilon_i|\mathbf{x}_i] = 0$. In this data generating process, the function of our interest is θ because obviously $\tau(\mathbf{x}_i) = \theta(\mathbf{x}_i)$, while h and u are not functions of our interest. Note that, Chernozhukov et al. (2018) assumed that θ is constant, i.e., independent of \mathbf{x}_i . However, as we discuss below, we can estimate θ similarly to Chernozhukov et al. (2018) even when that θ linearly depends on \mathbf{x}_i .

In this paper, we derive θ by a partialling-out approach as follows: we can re-write the structural equations as

$$y_i - \mathbb{E}[y_i|\mathbf{x}_i] = \theta(\mathbf{x}_i) \cdot (z_i - \mathbb{E}[z_i|\mathbf{x}_i]) + \varepsilon_i.$$

Here, define $q(\mathbf{x}_i) = \mathbb{E}[y_i|\mathbf{x}_i]$, where q belongs a convex subset \mathbb{Q} with some normed vector space. Then, the residuals for q and h are

$$\zeta_i = y_i - q(\mathbf{x}_i),$$

$$\eta_i = z_i - h(\mathbf{x}_i).$$

So we can obtain

$$\zeta_i = \theta(\mathbf{x}_i) \cdot \eta_i + \varepsilon_i. \tag{1}$$

Note that $\mathbb{E}[\zeta_i|\mathbf{x}_i] = 0$ because $\mathbb{E}[\eta_i|\mathbf{x}_i] = 0$ and $\mathbb{E}[\varepsilon_i|\mathbf{x}_i] = 0$.

We assume θ as a linear function with constant term such that

$$\theta(\mathbf{x}_i) = [1, \mathbf{x}_i^\top] \boldsymbol{\beta} = \beta^0 + x_i^1 \beta^1 + \dots + x_i^m \beta^m,$$

where $\boldsymbol{\beta} = [\beta^0, \dots, \beta^m]^\top \in \mathbb{R}^{m+1}$. Re-write (1) as

$$\zeta_i = \eta_i [1, \mathbf{x}_i^\top] \boldsymbol{\beta} + \varepsilon_i.$$

To derive $\boldsymbol{\beta}$, consider the following score vector:

$$\psi(\mathbf{x}_i; \hat{\boldsymbol{\beta}}, \hat{q}, \hat{h}) = [1, \mathbf{x}_i^\top]^\top (z_i - \hat{h}(\mathbf{x}_i))(y_i - \hat{q}(\mathbf{x}_i) - [1, \mathbf{x}_i^\top] \hat{\boldsymbol{\beta}}(z_i - \hat{h}(\mathbf{x}_i))). \tag{2}$$

Define the moment condition

$$\mathbb{E}[\psi(\mathbf{x}_i; \boldsymbol{\beta}, q, h)] = \mathbf{0}, \tag{3}$$

and Neyman–orthogonality (Chernozhukov et al., 2018)

$$\lim_{r \rightarrow 0} \frac{\partial}{\partial r} \mathbb{E}[\psi(\mathbf{x}_i; \boldsymbol{\beta}, q + r(q' - q), h + r(h' - h))] = \mathbf{0}, \tag{4}$$

where $r \in [0, 1)$, $q' \in \mathbb{Q}$ and $h' \in \mathbb{H}$. The Neyman–orthogonality implies first-order insensitivity to perturbations of the nuisance functions q and h . Then, we have Theorem 1, whose proof is in supplemental material D.

Theorem 1. *The score vector (2) satisfies both the moment condition (3) and Neyman–orthogonality (4).*

Given \hat{q} and \hat{h} , $\hat{\beta}$ can be obtained by solving (3) empirically from dataset as:

$$\sum_i \psi(\mathbf{x}_i; \hat{\beta}, \hat{q}, \hat{h}) = \sum_i \left(\hat{\eta}_i[1, \mathbf{x}_i^\top]^\top (\hat{\zeta}_i - \hat{\eta}_i[1, \mathbf{x}_i^\top] \hat{\beta}) \right) = \mathbf{0}. \quad (5)$$

(5) indicates that $\hat{\beta}$ is the solution of the regression problem from $\hat{\zeta}_i$ to $\hat{\eta}_i[1, \mathbf{x}_i^\top]$. That is

$$\hat{\beta} = \arg \min_{\beta'} \left(\sum_i \left(\hat{\zeta}_i - \hat{\eta}_i[1, \mathbf{x}_i^\top] \beta' \right)^2 \right).$$

The DML uses machine learning models to estimate q and h , and cross-fitting to reduce the effect of over-fitting on the estimation of parameter θ . In this paper, the data is split into two folds in cross-fitting. To derive the variance of $\hat{\beta}$, re-write (2) as

$$\psi(\mathbf{x}_i; \hat{\beta}, \hat{q}, \hat{h}) = \psi^a(\mathbf{x}_i; \hat{\beta}, \hat{q}, \hat{h}) \hat{\beta} + [1, \mathbf{x}_i^\top]^\top (z_i - \hat{h}(\mathbf{x}_i))(y_i - \hat{q}(\mathbf{x}_i)),$$

where

$$\psi^a(\mathbf{x}_i; \hat{h}) = (z_i - \hat{h}(\mathbf{x}_i))^2 [1, \mathbf{x}_i^\top]^\top [1, \mathbf{x}_i^\top].$$

From Theorem 3.2 in Chernozhukov et al. (2018), the asymptotic variance of $\sqrt{n}(\hat{\beta} - \beta)$ is

$$\hat{\sigma}^2 = \hat{J}^{-1} \frac{1}{K} \sum_{l=1}^L \frac{1}{|N_l|} \sum_{i \in N_l} \psi(\mathbf{x}_i; \hat{\beta}_l, \hat{q}_l, \hat{h}_l) \psi(\mathbf{x}_i; \hat{\beta}_l, \hat{q}_l, \hat{h}_l)^\top (\hat{J}^{-1})^\top \quad (6)$$

Here, \hat{q}_l and \hat{h}_l are the functions, and N_l is the set of subjects for fold l . Moreover,

$$\hat{J} = \frac{1}{L} \sum_{l=1}^L \frac{1}{|N_l|} \sum_{i \in N_l} \psi^a(\mathbf{x}_i; \hat{h}_l). \quad (7)$$

Then, the variance of $\hat{\beta}$ is

$$\text{Var}(\hat{\beta}) = \hat{\sigma}^2/n. \quad (8)$$

In summary, the DML procedure can be expressed as the following two steps. First, q and h are estimated from the two folds using machine learning models to obtain the estimated residuals: $\hat{\zeta}_i$ and $\hat{\eta}_i$. Second, β is estimated by regressing $\hat{\zeta}_i$ to $\hat{\eta}_i[1, \mathbf{x}_i^\top]$.

4 Method

We describe our method in this section. Prior to that, we explain the data distribution that our method focuses on. Let n be the number of subjects (sample size) in a dataset. Moreover, let $X = [\mathbf{x}_1, \dots, \mathbf{x}_n]^\top \in \mathbb{R}^{n \times m}$, $Z = [z_1, \dots, z_n]^\top \in \{0, 1\}^n$ and $Y = [y_1, \dots, y_n]^\top \in \mathbb{R}^n$ be the datasets of covariates, treatments, and outcomes, respectively. We consider that n subjects are partitioned horizontally into c parties, as follows:

$$X = \begin{bmatrix} X_1 \\ \vdots \\ X_c \end{bmatrix}, \quad Z = \begin{bmatrix} Z_1 \\ \vdots \\ Z_c \end{bmatrix}, \quad Y = \begin{bmatrix} Y_1 \\ \vdots \\ Y_c \end{bmatrix}.$$

The k th party has a partial dataset and corresponding treatments and outcomes, which are $X_k \in \mathbb{R}^{n_k \times m}$, $Z_k \in \{0, 1\}^{n_k}$, $Y_k \in \mathbb{R}^{n_k}$, where n_k is the number of subjects for each party in the k th row ($n = \sum_{k=1}^c n_k$).

This section proceeds as: we describe our method in Section 4.1, analyze the correctness of our method in Section 4.2, propose a dimension reduction method for DC-DML in Section 4.3, and finally discuss the advantages and disadvantages in Section 4.4.

4.1 DC-DML

Our method DC-DML is based on DC-QE (Kawamata et al., 2024) and DML (Chernozhukov et al., 2018), and enables to estimate CATE with privacy preservation of distributed data. As in Kawamata et al. (2024), DC-QE operates in two roles: user and analyst roles. Each user k have private covariates X_k , treatments Z_k and outcomes Y_k . DC-QE is conducted in three stages: construction of collaborative representations, estimation by the analyst, and estimation by the users. In the first stage, each user individually constructs intermediate representations and shares them with the analyst instead of the private dataset, then the analyst constructs the collaborative representations. In the sec-

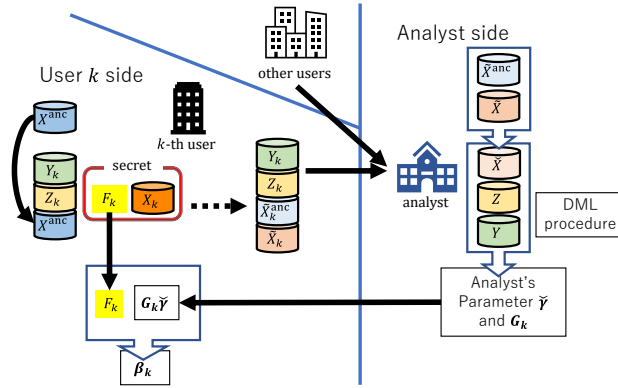


Figure 1: Overall illustration of the proposed method.

ond stage, the analyst estimates its own coefficients and variance using DML, and shares them with all users. In the final stage, each user calculates its own coefficients and variance. Each stage is described in turn from Section 4.1.1 to 4.1.3. Fig. 1 shows an overall illustration of DC-DML (The pseudo-code of DC-DML is in supplementary material B).

4.1.1 Construction of collaborative representations

In the first stage, construction of collaborative representations, we use the aggregation method proposed in Imakura and Sakurai (2020). First, users generate and share an anchor dataset $X^{\text{anc}} \in \mathbb{R}^{r \times m}$, which is a shareable dataset consisting of public or randomly constructed dummy data, where r is the number of subjects in the anchor data. The anchor dataset is used to compute the transformation matrices (described below as G_k) required to construct the collaborative representations. Second, each user k constructs intermediate representations using a linear row-wise dimensionality reduction function f_k such as principal component analysis (PCA) (Pearson, 1901), locality preserving projection (LPP) (He and Niyogi, 2003) and factor analysis (FA) (Spearman, 1904). f_k is consisting of a transformation matrix $F_k \in \mathbb{R}^{m \times \tilde{m}_k}$ and a shift vector $\mu_k \in \mathbb{R}^m$. $\tilde{m}_k (< m)$ is the reduced dimension of user k . μ_k is a mean vector in f_k with centering such as PCA and FA, or a zero vector in f_k without centering such as LPP. Then, the dimensionality reduction function

is applied as

$$\begin{aligned}\tilde{X}_k &= f_k(X_k) = (X_k - \mathbf{1}\boldsymbol{\mu}_k^\top)F_k \in \mathbb{R}^{n_k \times \tilde{m}_k}, \\ \tilde{X}_k^{\text{anc}} &= f_k(X^{\text{anc}}) = (X^{\text{anc}} - \mathbf{1}\boldsymbol{\mu}_k^\top)F_k \in \mathbb{R}^{r \times \tilde{m}_k},\end{aligned}$$

where $\mathbf{1} = [1, \dots, 1]^\top$. Moreover, f_k is private and can differ from other users. To consider the constant term in the linear CATE model, we combine $\mathbf{1}$ to \tilde{X}_k and \tilde{X}_k^{anc} . Formally, we can represent those as

$$\begin{aligned}[\mathbf{1}, \tilde{X}_k] &= [\mathbf{1}, X_k - \mathbf{1}\boldsymbol{\mu}_k^\top]\bar{F}_k, \\ [\mathbf{1}, \tilde{X}_k^{\text{anc}}] &= [\mathbf{1}, X^{\text{anc}} - \mathbf{1}\boldsymbol{\mu}_k^\top]\bar{F}_k,\end{aligned}$$

where

$$\bar{F}_k = \begin{bmatrix} 1 \\ F_k \end{bmatrix}.$$

Finally, each user k shares the intermediate representations $[\mathbf{1}, \tilde{X}_k]$ and $[\mathbf{1}, \tilde{X}_k^{\text{anc}}]$, treatments Z_k and outcomes Y_k to the analyst.

Next, the analyst transforms the shared intermediate representations into an common form called collaborative representations. To do this, the analyst computes the transformation functions for all k such that

$$[\mathbf{1}, \tilde{X}_k^{\text{anc}}]G_k \approx [\mathbf{1}, \tilde{X}_{k'}^{\text{anc}}]G_{k'} \in \mathbb{R}^{r \times \tilde{m}} \quad (k \neq k'),$$

where $G_k \in \mathbb{R}^{(\tilde{m}_k+1) \times \tilde{m}}$ and \tilde{m} is the dimension of collaborative representations. Then, we have the collaborative representation for k as

$$\check{X}_k = [\mathbf{1}, \tilde{X}_k]G_k \in \mathbb{R}^{n_k \times \tilde{m}}.$$

Let

$$[[\mathbf{1}, \tilde{X}_1^{\text{anc}}], \dots, [\mathbf{1}, \tilde{X}_c^{\text{anc}}]] = [U_1, U_2] \begin{bmatrix} \Sigma_1 & \\ & \Sigma_2 \end{bmatrix} \begin{bmatrix} V_1^\top \\ V_2^\top \end{bmatrix} \approx U_1 \Sigma_1 V_1^\top$$

be a low-rank approximation based on singular value decomposition of the matrix combining $[\mathbf{1}, \tilde{X}_k^{\text{anc}}]$, where $\Sigma_1 \in \mathbb{R}^{\tilde{m} \times \tilde{m}}$ is a diagonal matrix whose diagonal entries are the larger parts of the singular values and U_1 and V_1 are column orthogonal matrices whose columns are the corresponding left and right singular vectors, respectively. Matrix G_k is then computed as

$$G_k = \left([\mathbf{1}, \tilde{X}_k^{\text{anc}}]\right)^\dagger U_1,$$

where \dagger denotes the Moore–Penrose inverse. Then, the collaborative representations are given by

$$\check{X} = \begin{bmatrix} \check{X}_1 \\ \vdots \\ \check{X}_c \end{bmatrix} \in \mathbb{R}^{n \times \tilde{m}}.$$

4.1.2 Estimation by the analyst

In the second stage, estimation by the analyst, the analyst estimates their own CATE model based on the DML procedure that we described in Section 3. The analyst considers the data generation process as

$$y_i = \theta(\check{\mathbf{x}}_i) \cdot z_i + u(\check{\mathbf{x}}_i) + \varepsilon_i,$$

$$z_i = h(\check{\mathbf{x}}_i) + \eta_i,$$

and the linear CATE model as

$$\theta(\check{\mathbf{x}}_i) = \check{\mathbf{x}}_i^\top \boldsymbol{\gamma} = \check{x}_i^1 \gamma^1 + \cdots + \check{x}_i^{\tilde{m}} \gamma^{\tilde{m}},$$

where $\boldsymbol{\gamma} = [\gamma^1, \dots, \gamma^{\tilde{m}}]^\top \in \mathbb{R}^{\tilde{m}}$ and $\check{\mathbf{x}}_i$ is the collaborative representation of \mathbf{x}_i . The score vectors for the analyst are defined as

$$\check{\psi}(\check{\mathbf{x}}_i; \check{\boldsymbol{\gamma}}, \check{q}, \check{h}) = \check{\mathbf{x}}_i(z_i - \check{h}(\check{\mathbf{x}}_i))(y_i - \check{q}(\check{\mathbf{x}}_i) - \check{\mathbf{x}}_i^\top \check{\boldsymbol{\gamma}}(z_i - \check{h}(\check{\mathbf{x}}_i))),$$

$$\check{\psi}^a(\check{\mathbf{x}}_i; \check{h}) = (z_i - \check{h}(\check{\mathbf{x}}_i))^2 \check{\mathbf{x}}_i \check{\mathbf{x}}_i^\top.$$

where \check{q} and \check{h} are the analyst's functions, and $\check{\gamma} \in \mathbb{R}^{\check{m}}$ is the analyst's estimates.

The analyst's purpose in the second stage is to obtain $\check{\gamma}$. To accomplish this, first, the analyst constructs \check{q} and \check{h} from \check{X} , Z and Y using machine learning models to estimate residuals ζ_i and η_i . The estimated residuals are expressed as

$$\begin{aligned}\hat{\zeta}_i &= y_i - \check{q}(\check{\mathbf{x}}_i), \\ \hat{\eta}_i &= z_i - \check{h}(\check{\mathbf{x}}_i).\end{aligned}$$

Second, the analyst calculates $\check{\gamma}$ and $\text{Var}(\check{\gamma}) \in \mathbb{R}^{\check{m} \times \check{m}}$. $\check{\gamma}$ is the least squares solution of the following regression equation:

$$\hat{\zeta}_i = \hat{\eta}_i \check{\mathbf{x}}_i^\top \gamma + \varepsilon_i.$$

That is

$$\check{\gamma} = \arg \min_{\gamma'} \left(\sum_i \left(\hat{\zeta}_i - \hat{\eta}_i \check{\mathbf{x}}_i^\top \gamma' \right)^2 \right).$$

The analyst can calculate the variance of $\check{\gamma}$ in (6), (7) and (8), replacing ψ , ψ^a and $\hat{\beta}$ with $\check{\psi}$, $\check{\psi}^a$ and $\check{\gamma}$, respectively.

4.1.3 Estimation by the users

In the final stage, estimation by the users, the users estimates their own CATE model based on parameters that the analyst returns. The analysts's CATE model is written as

$$\begin{aligned}\check{X}_k \check{\gamma} &= [\mathbf{1}, \check{X}_k] G_k \check{\gamma} \\ &= [\mathbf{1}, X_k - \mathbf{1} \mu_k^\top] \bar{F}_k G_k \check{\gamma}.\end{aligned}$$

Then, for user k , subject i 's estimated CATE $\hat{\tau}_i$ is written as

$$\begin{aligned}\hat{\tau}_i &= \gamma_k^0 + (x_i^1 - \mu_k^1) \gamma_k^1 + \cdots + (x_i^m - \mu_k^m) \gamma_k^m \\ &= [1, -\mu_k^1, \cdots, -\mu_k^m] \gamma_k + \gamma_k^1 x_i^1 + \cdots + \gamma_k^m x_i^m \\ &= \alpha_k + \gamma_k^1 x_i^1 + \cdots + \gamma_k^m x_i^m\end{aligned} \tag{9}$$

where

$$\boldsymbol{\gamma}_k = [\gamma_k^0, \gamma_k^1, \dots, \gamma_k^m]^\top = \bar{F}_k G_k \check{\boldsymbol{\gamma}},$$

and

$$\alpha_k = [1, -\mu_k^1, \dots, -\mu_k^m] \boldsymbol{\gamma}_k. \quad (10)$$

For user k , α_k is a constant term and $\gamma_k^1, \dots, \gamma_k^m$ are coefficients for x_i^1, \dots, x_i^m in their CATE model. Thus, user k 's coefficients are expressed as $\boldsymbol{\beta}_k = [\alpha_k, \gamma_k^1, \dots, \gamma_k^m]^\top$.

The variance of $\boldsymbol{\gamma}_k$ is

$$\text{Var}(\boldsymbol{\gamma}_k) = \bar{F}_k G_k \text{Var}(\check{\boldsymbol{\gamma}}) G_k^\top \bar{F}_k^\top.$$

Then, the variance of α_k is

$$\text{Var}(\alpha_k) = [1, -\mu_k^1, \dots, -\mu_k^m] \text{Var}(\boldsymbol{\gamma}_k) \begin{bmatrix} 1 \\ -\mu_k^1 \\ \vdots \\ -\mu_k^m \end{bmatrix}. \quad (11)$$

User k can statistically test their CATE model if they obtains $\boldsymbol{\beta}_k$, $\text{Var}(\boldsymbol{\gamma}_k)$ and $\text{Var}(\alpha_k)$. To accomplish this, the following procedure is conducted in the final stage. First, the analyst returns $R_k^{\text{Point}} = G_k \check{\boldsymbol{\gamma}}$ and $R_k^{\text{Var}} = G_k \text{Var}(\check{\boldsymbol{\gamma}}) G_k^\top$ to user k . Then, user k calculates $\boldsymbol{\gamma}_k$ and $\text{Var}(\boldsymbol{\gamma}_k)$ as

$$\boldsymbol{\gamma}_k = \bar{F}_k R_k^{\text{Point}},$$

$$\text{Var}(\boldsymbol{\gamma}_k) = \bar{F}_k R_k^{\text{Var}} \bar{F}_k^\top.$$

Moreover, user k calculates α_k and $\text{Var}(\alpha_k)$ using (10) and (11), respectively. Then, user k obtained $\boldsymbol{\beta}_k$, $\text{Var}(\boldsymbol{\gamma}_k)$ and $\text{Var}(\alpha_k)$, and can test statistically $\boldsymbol{\beta}_k$.

For user k , subject i 's estimated CATE $\hat{\tau}_i$ are calculated from (9). To derive the variance of subject i 's CATE, re-write (9) as

$$\hat{\tau}_i = [1, x_i^1 - \mu_k^1, \dots, x_i^m - \mu_k^m] \boldsymbol{\gamma}_k$$

Then,

$$\text{Var}(\hat{\tau}_i) = [1, x_i^1 - \mu_k^1, \dots, x_i^m - \mu_k^m] \text{Var}(\boldsymbol{\gamma}_k) \begin{bmatrix} 1 \\ x_i^1 - \mu_k^1 \\ \vdots \\ x_i^m - \mu_k^m \end{bmatrix}.$$

Thus, user k can test $\hat{\tau}_i$ statistically based on $\text{Var}(\hat{\tau}_i)$.

4.2 Correctness of DC-DML

In this section, through a similar approach to Imakura et al. (2023), we discuss the correctness of DC-DML. Now, we consider the following subspace depending on k ,

$$\mathcal{S}_k = \mathcal{R}(\bar{F}_k G_k) \subset \mathbb{R}^{m+1}, \quad \dim(\mathcal{S}_k) = \check{m},$$

where \mathcal{R} denotes the range of a matrix. Define centralized analysis (CA) as collecting and analyzing the raw data, i.e., X , Z and Y , in one place. This is an ideal analysis, but not possible if the raw data contains private information. Then, we have Theorem 2, whose proof is in supplemental material E.

Theorem 2. *Let $\boldsymbol{\beta}_{\text{CA}}$ be the coefficients, and q_{CA} and h_{CA} be functions computed in CA.*

Moreover, consider $\boldsymbol{\gamma}_{\text{CA}} = [\gamma_{\text{CA}}^0, \gamma_{\text{CA}}^1, \dots, \gamma_{\text{CA}}^m]^\top$ such that

$$\gamma_{\text{CA}}^0 = [1, \mu_1^1, \dots, \mu_1^m] \boldsymbol{\beta}_{\text{CA}}, \quad \gamma_{\text{CA}}^j = \beta_{\text{CA}}^j \quad (j \neq 0).$$

If $\boldsymbol{\gamma}_{\text{CA}} \in \mathcal{S}_1 = \dots = \mathcal{S}_c$, $\boldsymbol{\mu}_1 = \dots = \boldsymbol{\mu}_c$, $\text{rank}(X^{\text{anc}} \bar{F}_k) = \check{m}$ for all $k \in \{1, \dots, c\}$, $q_{\text{CA}}(\mathbf{x}_i) = \check{q}(\check{\mathbf{x}}_i)$ and $h_{\text{CA}}(\mathbf{x}_i) = \check{h}(\check{\mathbf{x}}_i)$ for all $i \in \{1, \dots, n\}$, then $\boldsymbol{\beta}_{\text{CA}} = \boldsymbol{\beta}_k$.

Theorem 2 indicates that if the assumptions are satisfied, DC-DML can obtain the parameters computed in CA. Although it is unlikely that all of the assumptions are satisfied, Theorem 2 provides some hints for dimensionality reduction methods as we describe in Section 4.3.

4.3 A dimension reduction method for DC-DML

In this section, we propose a dimensionality reduction method for DC-DML with reference to Theorem 2. The dimensionality reduction method strongly affects the performance of DC-DML. In DC-DML, the coefficients γ_k is obtained from the subspace \mathcal{S}_k . If we could obtain γ_k close to γ_{CA} , we can achieve β_k close to β_{CA} . To accomplish this, the subspace \mathcal{S}_k should contain γ_{CA} .

Using an approach similar to Imakura et al. (2023), we consider a dimensionality reduction method for DC-DML (see supplementary material C for the pseudo-code). The basic idea of the approach is that each user k constructs F_k based on estimates of γ_{CA} obtained from their own local dataset. The estimate of γ_{CA} obtained by each user could be a good approximation of γ_{CA} . Thus, a bootstrap-based method can be a reasonable choice to achieve a good subspace. Let $0 < p < 1$ be a parameter for sampling rate. In the bootstrap-based method, first, through the DML procedure by a random samplings of size pn_k , user k obtains estimates of γ_{CA} as $\gamma_1, \dots, \gamma_{\tilde{m}_k}$. Then, user k constructs $F_k = [\bar{\gamma}_1, \dots, \bar{\gamma}_{\tilde{m}_k}]$, where $\bar{\gamma}_b \in \mathbb{R}^m$ is a vector excluding the first element of $\gamma_b \in \mathbb{R}^{m+1}$. The reason of excluding the first element of γ_b is that F_k should be a transformation matrix for m -dimensional covariates. However, since the first column of \bar{F}_k is $[1, 0, \dots, 0]^\top$ as in (4.1.1), the subspace contains the full range that the first element of γ_{CA} can take.

In addition, as with Imakura et al. (2023), the subspace can be constructed by combining multiple dimensionality reduction methods. Let $F_{BS} \in \mathbb{R}^{m \times \tilde{m}_{BS}}$ and $F_{DR} \in \mathbb{R}^{m \times \tilde{m}_{DR}}$ be the transformation matrices of the bootstrap-based and other methods, respectively, where $\tilde{m}_k = \tilde{m}_{BS} + \tilde{m}_{DR}$. Then, F_k is

$$F_k = [F_{BS}, F_{DR}].$$

4.4 Advantage and disadvantage

In this section, we describe the advantages and disadvantages of DC-DML. Those are attributed to DC-QE or DML with the linear CATE model described in Section 3.

There are four advantages. First, dimensionality reduction preserves the privacy of covariates. It is impossible to completely restore the raw data from the intermediate representations because of the dimensionality reduction. Moreover, by not sharing the dimensionality reduction function among users, even if others obtain a user’s intermediate representations, they cannot infer the user’s raw data. For more discussion for privacy preservation, refer to Imakura et al. (2021). Second, since DC-DML enables to collect a larger number of subjects from distributed data, it is possible to obtain better performance than in individual analysis. Third, DC-DML does not require repetitive communication (communication efficient). Finally, DC-DML is less susceptible to model mis-specification because it assumes a semi-parametric model.

Conversely, there are three disadvantages. First, DC-DML cannot be used directly if privacy information is included in the treatments or outcomes. Solutions to this issue include, for example, transforming treatments or outcomes into a format that preserves privacy through encryption and so on. Second, the performance of the resulting model may deteriorate because the dimensionality reduction reduces the information in the raw data. However, obtaining more subjects from the distributed data can improve performance more than the deterioration caused by dimensionality reduction. Finally, if the linear CATE model is not valid, i.e. non-linear, DC-DML may obtain incorrect conclusions.

5 Simulations

In this section we describe three simulations we conducted to demonstrate the effectiveness of DC-DML.¹ In Simulation I, that uses synthetic data, we show that DC-DML is useful in the setting of data distributions that would be incorrectly estimated by individual analysis (IA), the analysis performed by the user using only their own dataset. In Simulation II, that uses semi-synthetic data generated from the infant dataset, we compare the performances between DC-DML and other existing methods. In Simulation III, that uses real-world data from the financial assets and jobs datasets, we investigate the robustness of DC-DML performance in the presence of heterogeneous numbers of subjects or treatment group proportions per party.

In Simulation II, the methods to be compared to DC-DML are as follows. First are the DMLs in IA and CA, that we denote for convenience as IA-DML and CA-DML, respectively. As described above, IA-DML and CA-DML are, respectively, targets that DC-DML should perform better and closer to. Second, GRF and X-Learner in IA and CA, denoted for convenience with the prefixes IA- and CA-: IA-GRF, CA-GRF, IA-XL, and CA-XL. Finally, the distributed data analysis methods SR and FedCI.

In the simulations, we set up the machine learning models used in DML and X-learner as follows. First, both machine learning models used to estimate q and h in the DML methods (IA-DML, CA-DML and DC-DML) in the Simulation I are random forests. Second, the settings of the machine learning models used in Simulations II and III are as follows. We selected the machine learning models used to estimate q in the DML methods by our preliminary simulations from among five regression methods: multiple regression, random forests, K-nearest neighbor, light gradient boosting machine (LGBM) and support vector machine (SVM) with standardization. In the preliminary simulations for q , we repeated

¹We performed the simulations using Python codes, which are available from the corresponding author by reasonable request.

the regression of the outcomes on the covariates for the candidate methods in CA setting 50 times and set the criterion of selecting the one with the smallest root mean squared errors (RMSE) average. For h , similarly, we selected by preliminary simulations among five classification methods: logistic regression, random forests, K-nearest neighbor, LGBM and SVR. In our preliminary simulations for h , we followed the similar procedure as for q , where we set the criterion of selecting the one with the smallest average Brier score. Here, Brier Score is a mean squared error measure of probability forecasting. (Brier, 1950) The hyperparameters for the candidate methods were the default values shown in supplemental material F. As a result of our preliminary simulations, we chose SVM as the machine learning models to be used in the estimation of q and h , both in Simulation II. For the financial data set in Simulation III, we set q and h to multiple regression and logistic regression, respectively. For the jobs dataset, we set q and h to multiple regression and random forest, respectively. We use the same models for the outcome and propensity score in X-Learner (IA-XL and CA-XL) as in DML in all simulations. The results of the preliminary simulations are in supplemental material G.

The settings used in DC-DML are as follows. As the intermediate representation construction methods, we used six: PCA, LPP, FA, PCA+B, LPP+B, and FA+B. Here, +B represents the combination with the bootstrap-based dimensionality reduction method. The intermediate representation dimension and collaborative representation dimension were set as $\tilde{m}_k = m - 1$ for all k and $\tilde{m} = m$, respectively. In combination with the bootstrap-based dimensionality reduction method, the BS dimension was set to three in Simulation I and $\lceil 0.1m \rceil$ in Simulation II and III. Here, $\lceil \cdot \rceil$ is the ceiling function. Anchor data were generated from uniform random numbers of maximum and minimum values for each covariate and their subject number r was the same of the original dataset X .

As described below, in Simulation II, we used the five methods described in Section 2 as comparison methods: DML, GRF, X-Learner, SR and FedCI. Also, in Simulation III, we

used DML and SR as comparison methods. See supplemental material H for the detailed settings of those methods.

In Simulations II and III, the evaluation measures used were how close the estimates were to the benchmarks. The benchmarks in Simulations II and III were the true values and the average values of 50 trials of CA-DML, respectively. In this study, we consider four evaluation measures: the RMSE of CATE, the consistency rate of significance of CATE, the RMSE of coefficients, and the consistency rate of significance of coefficients. Note that, for reasons of space limitation, results other than the RMSE of CATE in Simulation III were shown in the supplementary material I.

The RMSE of CATE

The RMSE of CATE is a measure of how much the predicted CATE matched the benchmark CATE as

$$\sqrt{\frac{1}{N} \sum_i (\tau_{i,\text{BM}} - \hat{\tau}_i)^2},$$

where $\tau_{i,\text{BM}}$ is the benchmark CATE and $\hat{\tau}_i$ is the estimated CATE. The lower this measure, the better.

The consistency rate of significance of CATE

The consistency rate of significance of CATE is the rate where the estimated CATE obtained a statistical test result of “significantly positive,” “significantly negative,” or “not significant” in 5% level when the benchmark CATE is positive, negative, or zero, respectively. For Simulation III, we set the benchmark CATE is positive, negative, or zero when the estimate in CA-DML is significantly positive, significantly negative or not significant, respectively, in 5% level. The higher this measure, the better. This measure was not calculated in X-Learner and FedCI, because statistical testing methods for CATE are not

provided in those methods.

The RMSE of coefficients

The RMSE of coefficients is a measure of how much the estimated coefficients matched that of the benchmark as

$$\sqrt{\frac{1}{m+1} \sum_j (\beta_{\text{BM}}^j - \beta_k^j)^2},$$

where β_{BM}^j is the benchmark coefficient. The lower this measure, the better. Since GRF, X-Learner and FedCI are not models that estimate linear CATE, this measure was not calculated in those models.

The consistency rate of significance of coefficients

The consistency rate of significance of coefficients is the rate where the estimated coefficient obtained a statistical test result of “significantly positive,” “significantly negative,” or “not significant” in 5% level when the benchmark coefficient is positive, negative, or zero, respectively. For Simulation III, we set the benchmark coefficient is positive, negative, or zero when the estimate in CA-DML is significantly positive, significantly negative or not significant, respectively, in 5% level. The higher this measure, the better. As with the RMSE of coefficients, this measure was not calculated in GRF, X-Learner and FedCI.

5.1 Simulation I: Proof of concepts in synthetic data

In Simulation I, we considered the situation where two parties ($c = 2$) each had a dataset consisting of 300 subjects ($n_k = 300$) and 10 covariates ($m = 10$). The covariates x_i^1 and x_i^2 were distributed as in Figure 2, where blue and orange markers represent that of party 1 and 2, respectively. The other covariates were drawn from a normal distribution $\mathcal{N}(0, 1)$.

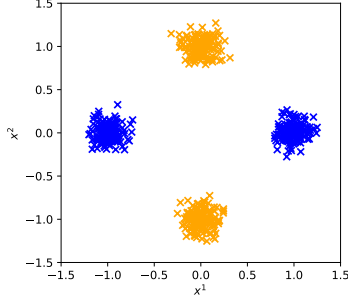


Figure 2: The data distribution in Simulation I. The blue and orange markers represent the covariates of party 1 and 2, respectively.

The setting of the data generation process in Simulation I was

$$\begin{aligned} \theta(\mathbf{x}_i) &= 1 + x_i^1 + x_i^2, \\ u(\mathbf{x}_i) &= |x_i^1| + |x_i^2|, \\ h(\mathbf{x}_i) &= \frac{1}{1 - \exp(-x_i^1 - x_i^2)}, \\ \varepsilon_i &\sim \mathcal{N}(0, 0.1), \\ \eta_i &= \begin{cases} 1 - h(\mathbf{x}_i) & \text{w.p. } h(\mathbf{x}_i) \\ -h(\mathbf{x}_i) & \text{w.p. } 1 - h(\mathbf{x}_i) \end{cases} \end{aligned}$$

where w.p. is “with probability”. In this setting, the constant term and the coefficients of x_i^1 and x_i^2 should be estimated to be significantly one.

Party 1 has the dataset with the broad distribution for covariate 1 and the narrow distribution for covariate 2. Thus, party 1 would be able to estimate the coefficient of covariate 1 relatively correctly in IA-DML, but would have difficulty estimating the coefficient of covariate 2. For party 2, the opposite of party 1 can be said.

The result of Simulation I is shown in Table 2. In CA-DML, the constant term and the coefficients of x_i^1 and x_i^2 are significant and close to their true values, and the coefficients of the other covariates are not significant. Thus, CA-DML obtained reasonable estimation results. Conversely, IA-DML obtained some wrong estimation results in both parties.

Covariates	CA-DML		IA-DML			DC-DML(PCA+B)				
			Party 1		Party 2	Party 1		Party 2		
const.	1.0283	**	0.6300	**	1.0068	**	0.9563	**	1.0207	**
x^1	1.0610	**	0.9952	**	0.6950		1.0578	**	1.0119	**
x^2	1.1290	**	2.0799		1.0359	**	0.9042	**	0.9761	**
x^3	-0.1628		-0.1161		-0.3211	*	-0.0961		-0.1269	
x^4	-0.1595		-0.0220		-0.0021		-0.1489		-0.1264	
x^5	0.0566		-0.0924		0.1679		0.0147		0.0190	
x^6	0.0905		0.3367	*	-0.2482		0.1608		0.1354	
x^7	-0.0434		0.0771		-0.1849		-0.0317		-0.0960	
x^8	-0.0494		-0.0397		-0.1370		-0.0336		-0.0065	
x^9	0.0607		-0.0955		0.1867		0.0418		0.0536	
x^{10}	-0.1773		-0.2022		-0.0543		-0.1270		-0.1391	

** $p < 0.01$, * $p < 0.05$

Table 2: The result of Simulation I.

DC-DML conducted by the PCA+B dimensionality reduction method obtained estimation results similar to CA-DML. This result suggests that even in situations where it is difficult to make valid estimates using IA-DML, DC-DML can produce more valid estimates than that.

5.2 Simulation II: Comparison with other methods in semi-synthetic data

In Simulation II, we evaluate the performance of DC-DML on semi-synthetic data generated from the infant health and development program (IHDP) dataset. The IHDP dataset

is “a randomized simulation that began in 1985, targeted low-birth-weight, premature infants, and provided the treatment group with both intensive high-quality child care and home visits from a trained provider.” (Hill, 2011) ² The IHDP dataset is consisting of 25 covariates and a treatment variable and does not include an outcome variable. Thus, the outcomes needs to be synthetically set up for the simulation. Hill (2011) removed data on all children with nonwhite mothers from the treatment group to imbalance the covariates in the treatment and control groups. We followed this as well, and as a result, the dataset in Simulation II consisted of 139 subjects in the treatment group and 608 subjects in the control group.

In Simulation II, we considered the situation where three parties ($c = 3$) each had a dataset consisting of 249 subjects ($n_k = 249$) and 25 covariates ($m = 25$). The ratios of treatment groups were equal in all parties. The outcome variable in Simulation II we set as

$$\begin{aligned}\theta(\mathbf{x}_i) &= \text{const.} + \mathbf{x}_i^\top \boldsymbol{\beta}, \\ \boldsymbol{\beta} &= \left[\frac{1}{\sigma^1}, 0, -\frac{1}{\sigma^3}, \frac{1}{\sigma^4}, 0, -\frac{1}{\sigma^6}, \dots \right]^\top, \\ \text{const.} &= -\mathbf{x}_i^\top [1, 0, -1, 1, 0, -1, \dots]^\top \\ u(\mathbf{x}_i) &= \left| \frac{x_i^1 - \bar{x}^1}{\sigma^1} \right| + \dots + \left| \frac{x_i^m - \bar{x}^m}{\sigma^m} \right|, \\ \varepsilon_i &\sim \mathcal{N}(0, 0.1),\end{aligned}$$

where \bar{x}^j and σ^j are the average of and standard deviation of covariate j , respectively, in the dataset. Note that, $h(\mathbf{x}_i)$ and η_i were not defined because the treatments were included in the dataset.

The results of the four evaluation measures in Simulation II is shown in Figures 3(a)-3(d). In this simulation, we conducted 50 simulations with different random seed values

²The IHDP dataset is published as the supplementary file (<https://www.tandfonline.com/doi/abs/10.1198/jcgs.2010.08162>).

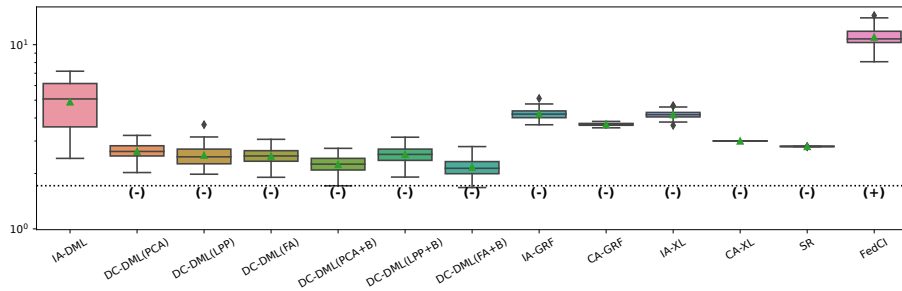
for data distributing and machine learning. The symbols + and – in parentheses in the figures represent significant positive and significant negative differences from the IA-DML results, respectively, in t -test. There were no methods that were not significantly different from DC-DML.

As described below, Figures 3(a)-3(d) show that DC-DML performs well for each of the evaluation measures in Simulation 2. First, as shown in Figure 3(a), the result for the RMSE of CATE shows that DC-DML significantly outperformed IA-DML. Moreover, DC-DML obtained better result than the existing methods. Second, as shown in Figure 3(b), the result for the consistency rate of significance of CATE shows that DC-DML significantly outperformed IA-DML. Moreover, DC-DML obtained better result than the existing methods. Third, as shown in Figure 3(c), the result for the RMSE of coefficients shows that DC-DML significantly outperformed IA-DML and are comparable to CA-DML and SR. Finally, as shown in Figure 3(d), the result for the consistency rate of significance of coefficients shows that DC-DML significantly outperformed IA-DML. Moreover, DC-DML obtained better result than SR. These results in Simulation II suggests that DC-DML can outperform IA-DML and obtain equal or better results than the existing methods.

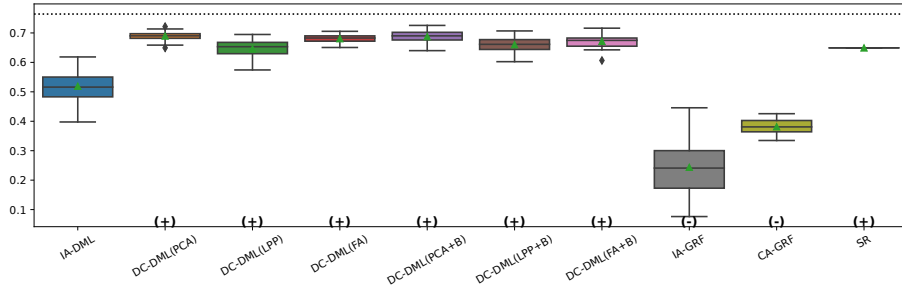
5.3 Simulation III: Robustness to distribution settings in real-world data

Based on real-world datasets of financial assets and jobs, in Simulation III, we investigate the robustness of DC-DML performance in the case where the number of subjects or rate of treatment group across parties is imbalanced. As the financial assets dataset, we focused on the SIPP dataset, which was used in Chernozhukov et al. (2018) to estimate the effect of 401(k) eligibility on accumulated assets.³ The SIPP dataset consists of 9915 observations

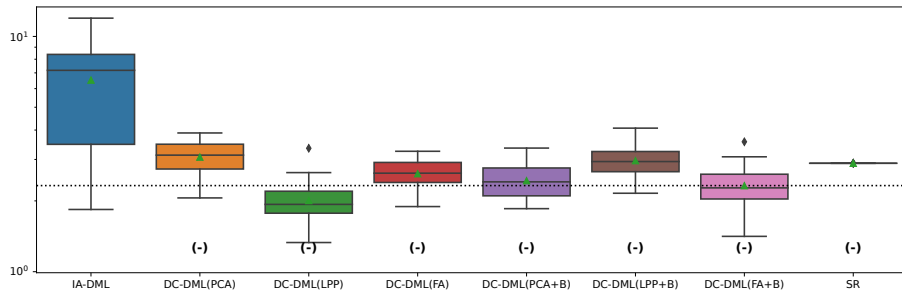
³This is available from the repository of Chernozhukov et al. (2018) (<https://github.com/VC2015/DMLonGitHub/>).



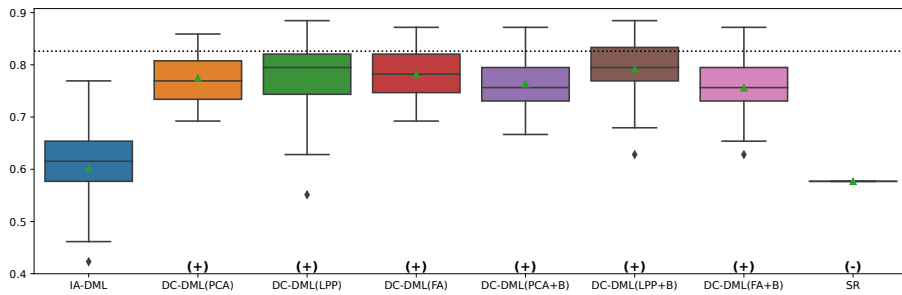
(a) The RMSE of CATE



(b) The consistency rate of significance of CATE



(c) The RMSE of coefficients



(d) The consistency rate of significance of coefficients

Figure 3: Results of Simulation II. The dashed line is the average of CA-DML results. The triangle markers represent their average values. The vertical axes in Figures 3(a) and 3(c) are the logarithmic scales.

		setting A			setting B			setting C		
subjects		even			even			uneven		
treatment rate		even			uneven			even		
dataset	party	all	treated	controlled	all	treated	controlled	all	treated	controlled
financial assets	1	3304	1227	2077	3304	2549	755	6864	2549	4315
	2	3304	1227	2077	3304	849	2455	2287	849	1438
	3	3304	1227	2077	3304	283	3021	762	283	479
jobs	1	891	61	830	891	92	799	1337	92	1245
	2	891	61	830	891	61	830	891	61	830
	3	891	61	830	891	30	861	445	30	415

Table 3: The number of subjects in each setting for Simulation III.

and includes nine individual information (age, inc, educ, fsize, marr, twoearn, db, pira, hown) as covariates, 401(k) offerings as treatments, and net financial assets as outcomes. As the jobs dataset, we focused on Dehejia and Wahba (1999)’s dataset, which was used to estimate the treatment effects of work experience and counseling on incomes.⁴ The jobs dataset consists of 2675 observations and includes eight individual information (age, black, hispanic, married, no degree, re74) as covariates, trainings as treatments, and real earnings in 1978 as outcomes.

In Simulation III, we considered three parties ($c = 3$) and three settings for data distribution where the rate of treatment group and the number of subjects are even or uneven, as shown in Table 3. In setting A, all parties have the same number of subjects and the same rate of treatment groups. In setting B, the number of subjects is even, but the rate of treatment groups differs across parties. In setting C, the number of subjects differs, but the rate of treatment groups is even across parties.

In Simulation III, the result of CA-DML is used as the benchmark. Table 4 shows the average results of 50 trials of CA-DML. Note that, comparisons with GRF, X-Learner, and

⁴This is available from the author’s website (<https://users.nber.org/~rdehejia/nswdata.html>).

financial assets		jobs	
covariate	coefficient	covariate	coefficient
const.	-9705.1794	const.	-7533.7519
age	172.0307	age	226.4912 *
inc	-0.1297	black	2493.7939
educ	642.9040	hispanic	1519.3141
fsize	-1003.0686	married	-2215.7011
marr	1102.9090	no_degree	-858.5624
twoearn	5607.3989	re74	-0.3354
db	5657.7264 *		
pira	-1032.3599		
hown	5324.2854 *		

* $p < 0.05$

Table 4: The benchmark coefficients of Simulation III.

FedCI do not make sense because those assume the non-linear CATE model. Thus, only CA-DML, IA-DML and SR were considered as comparison with DC-DML.

Figure 4 represents the RMSE of CATE in Simulation III for the financial assets dataset. The symbols +, - and 0 in parentheses in the figures represent significant positive, significant negative and not significant differences from the IA-DML results, respectively, in t -test. The results for parties 1, 2 and 3 are shown on the left, middle and right sides, respectively, in the figures. In all cases shown in Figure 4, DC-DML results are better than IA-DML and SR. In addition, the dimensionality reduction method combined with bootstrapping shows robust results. However, DC-DML using LPP are relatively worse than for DC-DML using the other dimensionality reduction methods. No SR results are

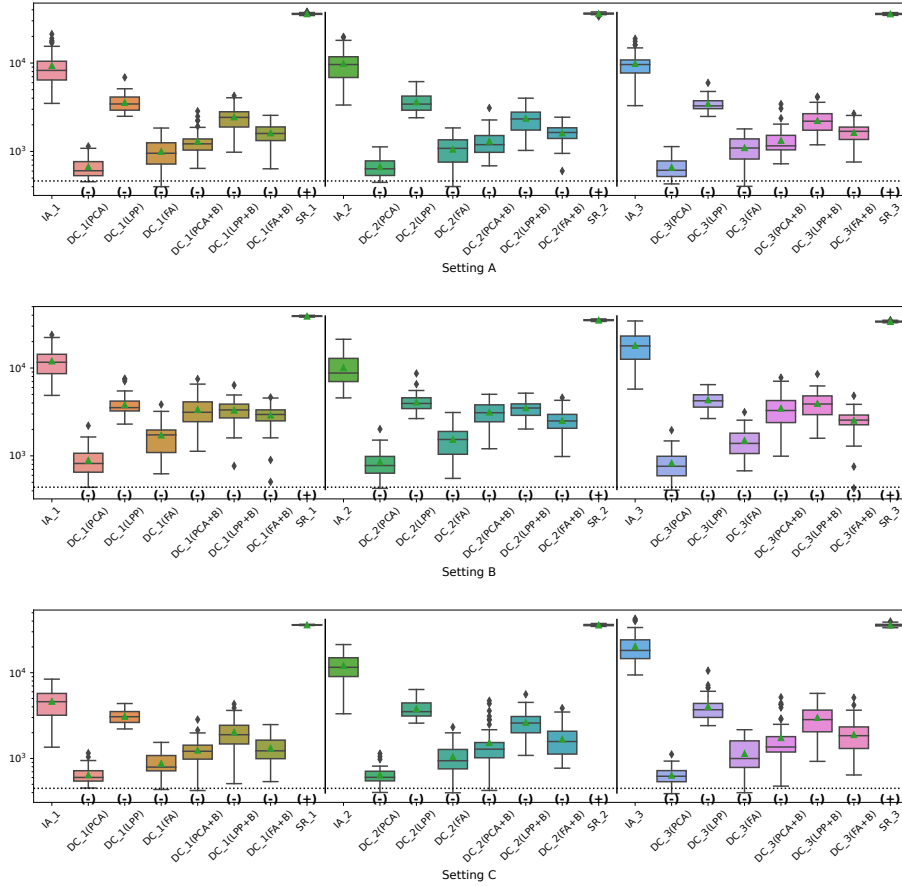


Figure 4: The RMSE of CATE in Simulation III for the financial assets dataset. The dashed line is the average of CA-DML results. The triangle markers represent their average values. The vertical axis is the logarithmic scale.

better than IA-DML.

Figure 5 represents the RMSE of CATE in Simulation III for the jobs dataset. Similar to the simulation for the financial assets, DC-DML results are better than IA-DML and SR in all cases in Figure 5. Although, as shown in supplementary material I, DC-DML does not always exhibits better performance than IA-DML in the other measures, DC-DML results are often better than IA-DML. As with the financial assets dataset, the dimensionality reduction method combined with bootstrapping shows robust results, and SR results are often worse than IA-DML.

The simulation results in both datasets suggest that the choice of dimensionality reduc-

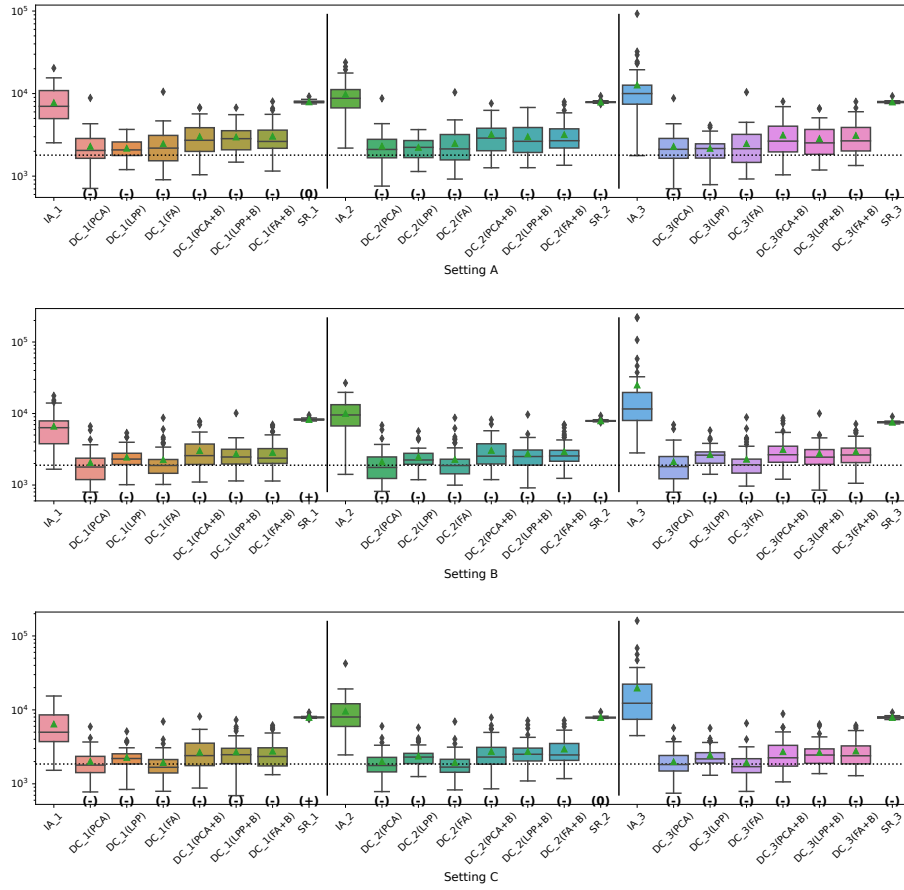


Figure 5: The RMSE of CATE in Simulation III for the jobs dataset. The meaning of symbols, lines and axes are the same with Figure 4.

tion method has a significant impact on the performance of DC-DML. What dimensionality reduction method provides good performance for DC-DML is likely to be data-dependent. How to select a dimensionality reduction method is a future issue.

On summary, in Simulation III with two datasets, DC-DML achieved better results than IA-DML, although not in all cases. Those results suggest that DC-DML can obtain comparable results to CA-DML in various data distribution settings than in IA-DML.

6 Conclusion

Utilizing distributed data across multiple parties is an important topic in data science, but privacy concerns need to be addressed. In this study, we proposed DC-DML that can estimate CATEs while preserving the privacy of distributed data. Our method enables flexible estimation of CATE models from distributed data through a semi-parametric approach and does not require iterative communication. Through the three simulations, we demonstrated the effectiveness of our method as follows. First, even in situations where it is difficult to make valid estimates using IA-DML, DC-DML can produce more valid estimates than that. Second, DC-DML can outperform IA-DML and obtain equal or better results than the existing methods. Third, DC-DML can obtain comparable results to CA-DML in various data distribution settings than in IA-DML.

Our study has some limitations. First, our method assumes the linear CATE model. As mentioned in Section 4.4, the linear CATE model may obtain incorrect conclusions in data where the assumption is not valid. To address this issue, it is necessary to extend our method to a method that can assume a non-linear CATE model. Second, it is not clear how the dimensionality reduction method should be selected in DC-DML. Addressing these issues is a future study.

References

- Athey, S., J. Tibshirani, and S. Wager (2019). Generalized random forests. *The Annals of Statistics* 47(2), 1148.
- Bia, M., M. Huber, and L. Laff ers (2023). Double machine learning for sample selection models. *Journal of Business & Economic Statistics*, 1–12.
- Bogdanova, A., A. Nakai, Y. Okada, A. Imakura, and T. Sakurai (2020). Federated learning

- system without model sharing through integration of dimensional reduced data representations. In *Proceedings of IJCAI 2020 International Workshop on Federated Learning for User Privacy and Data Confidentiality*.
- Brier, G. W. (1950). Verification of forecasts expressed in terms of probability. *Monthly weather review* 78(1), 1–3.
- Chernozhukov, V., D. Chetverikov, M. Demirer, E. Duflo, C. Hansen, W. Newey, and J. Robins (2018, 01). Double/debiased machine learning for treatment and structural parameters. *The Econometrics Journal* 21(1), C1–C68.
- Dehejia, R. H. and S. Wahba (1999). Causal effects in nonexperimental studies: Reevaluating the evaluation of training programs. *Journal of the American statistical Association* 94(448), 1053–1062.
- Engle, R. F., C. W. J. Granger, J. Rice, and A. Weiss (1986). Semiparametric estimates of the relation between weather and electricity sales. *Journal of the American statistical Association* 81(394), 310–320.
- Fan, Q., Y. Hsu, R. P. Lieli, and Y. Zhang (2022). Estimation of conditional average treatment effects with high-dimensional data. *Journal of Business & Economic Statistics* 40(1), 313–327.
- He, X. and P. Niyogi (2003). Locality preserving projections. *Advances in neural information processing systems* 16.
- Hill, J. L. (2011). Bayesian nonparametric modeling for causal inference. *Journal of Computational and Graphical Statistics* 20(1), 217–240.
- Imakura, A., A. Bogdanova, T. Yamazoe, K. Omote, and T. Sakurai (2021). Accuracy and

- privacy evaluations of collaborative data analysis. In *The Second AAAI Workshop on Privacy-Preserving Artificial Intelligence (PPAI-21)*.
- Imakura, A., H. Inaba, Y. Okada, and T. Sakurai (2021). Interpretable collaborative data analysis on distributed data. *Expert Systems with Applications* 177, 114891.
- Imakura, A. and T. Sakurai (2020). Data collaboration analysis framework using centralization of individual intermediate representations for distributed data sets. *ASCE-ASME Journal of Risk and Uncertainty in Engineering Systems, Part A: Civil Engineering* 6(2), 04020018.
- Imakura, A., R. Tsunoda, R. Kagawa, K. Yamagata, and T. Sakurai (2023). DC-COX: Data collaboration cox proportional hazards model for privacy-preserving survival analysis on multiple parties. *Journal of Biomedical Informatics* 137, 104264.
- Imbens, G. W. and D. B. Rubin (2015). *Causal inference in statistics, social, and biomedical sciences*. Cambridge University Press.
- Karr, A. F., X. Lin, A. P. Sanil, and J. P. Reiter (2005). Secure regression on distributed databases. *Journal of Computational and Graphical Statistics* 14(2), 263–279.
- Kawamata, Y., R. Motai, Y. Okada, A. Imakura, and T. Sakurai (2024). Collaborative causal inference on distributed data. *Expert Systems with Applications* 244, 123024.
- Konečný, J., H. B. McMahan, F. X. Yu, P. Richtárik, A. T. Suresh, and D. Bacon (2016). Federated learning: Strategies for improving communication efficiency. In *NIPS Workshop on Private Multi-Party Machine Learning*.
- Künzel, S. R., J. S. Sekhon, P. J. Bickel, and B. Yu (2019). Metalearners for estimating heterogeneous treatment effects using machine learning. *Proceedings of the national academy of sciences* 116(10), 4156–4165.

- McMahan, B., E. Moore, D. Ramage, S. Hampson, and B. A. y Arcas (2017). Communication-efficient learning of deep networks from decentralized data. In *Artificial intelligence and statistics*, pp. 1273–1282. PMLR.
- Pearson, K. (1901). LIII. on lines and planes of closest fit to systems of points in space. *The London, Edinburgh, and Dublin philosophical magazine and journal of science* 2(11), 559–572.
- Rosenbaum, P. R. and D. B. Rubin (1983). The central role of the propensity score in observational studies for causal effects. *Biometrika* 70(1), 41–55.
- Spearman, C. (1904). “general intelligence,” objectively determined and measured. *The American Journal of Psychology* 15(2), 201–292.
- Tan, X., C. H. Chang, L. Zhou, and L. Tang (2022). A tree-based model averaging approach for personalized treatment effect estimation from heterogeneous data sources. In *International Conference on Machine Learning*, pp. 21013–21036. PMLR.
- Vo, T. V., Y. Lee, T. N. Hoang, and T.-Y. Leong (2022). Bayesian federated estimation of causal effects from observational data. In *The 38th Conference on Uncertainty in Artificial Intelligence*.
- Wu, S., D. Huang, and H. Wang (2023). Network gradient descent algorithm for decentralized federated learning. *Journal of Business & Economic Statistics* 41(3), 806–818.
- Xiong, R., A. Koenecke, M. Powell, Z. Shen, J. T. Vogelstein, and S. Athey (2023). Federated causal inference in heterogeneous observational data. *Statistics in Medicine* 42(24), 4418–4439.

SUPPLEMENTARY MATERIAL

A Algorithm of data collaboration quasi-experiment

Algorithm 1 is the pseudo-code of data collaboration quasi-experiment (DC-QE).

B Algorithm of data collaboration double machine learning

Algorithm 2 is the pseudo-code of data collaboration double machine learning (DC-DML).

C Algorithm of the bootstrap-based dimensionality reduction for DC-DML

Algorithm 3 is the pseudo-code of the bootstrap-based dimensionality reduction for DC-DML.

D The proof of Theorem 1

Proof. Denote $\bar{\mathbf{x}}_i = [1, \mathbf{x}_i^\top]^\top$. First, we can prove the moment condition as

$$\begin{aligned}\mathbb{E}[\psi(\mathbf{x}_i; \boldsymbol{\beta}, q, h)] &= \mathbb{E} [\bar{\mathbf{x}}_i(z_i - h(\mathbf{x}_i))(y_i - q(\mathbf{x}_i) - \bar{\mathbf{x}}_i^\top \boldsymbol{\beta}(z_i - h(\mathbf{x}_i)))] \\ &= \mathbb{E} [\bar{\mathbf{x}}_i \eta_i \varepsilon_i] \\ &= \mathbb{E} [\bar{\mathbf{x}}_i \mathbb{E} [\eta_i \varepsilon_i | \mathbf{x}_i]] \\ &= \mathbf{0}.\end{aligned}$$

Second, for the Neyman–orthogonality, consider

$$\begin{aligned}
& \psi(\mathbf{x}_i; \boldsymbol{\beta}, q + r\delta_q, h + r\delta_h) \\
&= \bar{\mathbf{x}}_i(z_i - h(\mathbf{x}_i) - r\delta_h(\mathbf{x}_i))(y_i - q(\mathbf{x}_i) - r\delta_q(\mathbf{x}_i) - \bar{\mathbf{x}}_i^\top \boldsymbol{\beta}(z_i - h(\mathbf{x}_i) - r\delta_h(\mathbf{x}_i))) \\
&= \bar{\mathbf{x}}_i(\eta_i - r\delta_h(\mathbf{x}_i))(\zeta_i - r\delta_q(\mathbf{x}_i) - \bar{\mathbf{x}}_i^\top \boldsymbol{\beta}(\eta_i - r\delta_h(\mathbf{x}_i))) \\
&= \bar{\mathbf{x}}_i \{ (\eta_i - r\delta_h(\mathbf{x}_i))(\eta_i - r\delta_q(\mathbf{x}_i)) - \bar{\mathbf{x}}_i^\top \boldsymbol{\beta}(\eta_i - r\delta_h(\mathbf{x}_i))^2 \},
\end{aligned}$$

where $\delta_h = h' - h$ and $\delta_q = q' - q$. Then,

$$\begin{aligned}
& \lim_{r \rightarrow 0} \frac{\partial}{\partial r} \mathbb{E} [\psi(\mathbf{x}_i; \boldsymbol{\beta}, q + r\delta_q, h + r\delta_h)] \\
&= \lim_{r \rightarrow 0} \frac{\partial}{\partial r} \mathbb{E} [\bar{\mathbf{x}}_i \mathbb{E} [\{ (\eta_i - r\delta_h(\mathbf{x}_i))(\zeta_i - r\delta_q(\mathbf{x}_i)) - \bar{\mathbf{x}}_i^\top \boldsymbol{\beta}(\eta_i - r\delta_h(\mathbf{x}_i))^2 \} | \mathbf{x}_i]] \\
&= \mathbb{E} \left[\bar{\mathbf{x}}_i \lim_{r \rightarrow 0} \frac{\partial}{\partial r} \mathbb{E} [\{ (\eta_i - r\delta_h(\mathbf{x}_i))(\zeta_i - r\delta_q(\mathbf{x}_i)) - \bar{\mathbf{x}}_i^\top \boldsymbol{\beta}(\eta_i - r\delta_h(\mathbf{x}_i))^2 \} | \mathbf{x}_i] \right].
\end{aligned}$$

Here,

$$\begin{aligned}
& \lim_{r \rightarrow 0} \frac{\partial}{\partial r} \mathbb{E} [\{ (\eta_i - r\delta_h(\mathbf{x}_i))(\zeta_i - r\delta_q(\mathbf{x}_i)) - \bar{\mathbf{x}}_i^\top \boldsymbol{\beta}(\eta_i - r\delta_h(\mathbf{x}_i))^2 \} | \mathbf{x}_i] \\
&= \lim_{r \rightarrow 0} \frac{\partial}{\partial r} \mathbb{E} [(\eta_i - r\delta_h(\mathbf{x}_i))(\zeta_i - r\delta_q(\mathbf{x}_i)) | \mathbf{x}_i] - \lim_{r \rightarrow 0} \frac{\partial}{\partial r} \mathbb{E} [\bar{\mathbf{x}}_i^\top \boldsymbol{\beta}(\eta_i - r\delta_h(\mathbf{x}_i))^2 | \mathbf{x}_i].
\end{aligned}$$

The first term is

$$\begin{aligned}
& \lim_{r \rightarrow 0} \frac{\partial}{\partial r} \mathbb{E} [(\eta_i - r\delta_h(\mathbf{x}_i))(\zeta_i - r\delta_q(\mathbf{x}_i)) | \mathbf{x}_i] \\
&= \lim_{r \rightarrow 0} \mathbb{E} [-\eta_i \delta_q(\mathbf{x}_i) - \zeta_i \delta_h(\mathbf{x}_i) + 2r\delta_h(\mathbf{x}_i)\delta_q(\mathbf{x}_i) | \mathbf{x}_i] \\
&= \mathbb{E} [-\eta_i \delta_q(\mathbf{x}_i) - \zeta_i \delta_h(\mathbf{x}_i) | \mathbf{x}_i] \\
&= -\delta_q(\mathbf{x}_i) \mathbb{E} [\eta_i | \mathbf{x}_i] - \delta_h(\mathbf{x}_i) \mathbb{E} [\zeta_i | \mathbf{x}_i] \\
&= \mathbf{0},
\end{aligned}$$

and the second term is

$$\begin{aligned}
& \lim_{r \rightarrow 0} \frac{\partial}{\partial r} \mathbb{E} [\bar{\mathbf{x}}_i^\top \boldsymbol{\beta} (\eta_i - r \delta_h(\mathbf{x}_i))^2 | \mathbf{x}_i] \\
&= \bar{\mathbf{x}}_i^\top \boldsymbol{\beta} \lim_{r \rightarrow 0} \frac{\partial}{\partial r} \mathbb{E} [(\eta_i - r \delta_h(\mathbf{x}_i))^2 | \mathbf{x}_i] \\
&= \bar{\mathbf{x}}_i^\top \boldsymbol{\beta} \lim_{r \rightarrow 0} \mathbb{E} [-2(\eta_i - r \delta_h(\mathbf{x}_i)) \delta_h(\mathbf{x}_i) | \mathbf{x}_i] \\
&= -2 \bar{\mathbf{x}}_i^\top \boldsymbol{\beta} \delta_h(\mathbf{x}_i) \lim_{r \rightarrow 0} \mathbb{E} [(\eta_i - r \delta_h(\mathbf{x}_i)) | \mathbf{x}_i] \\
&= -2 \bar{\mathbf{x}}_i^\top \boldsymbol{\beta} \delta_h(\mathbf{x}_i) \mathbb{E} [\eta_i | \mathbf{x}_i] \\
&= \mathbf{0}.
\end{aligned}$$

Thus,

$$\lim_{r \rightarrow 0} \frac{\partial}{\partial r} \mathbb{E} [\psi(\mathbf{x}_i; \boldsymbol{\beta}, q + r \delta_q, h + r \delta_h)] = \mathbf{0}.$$

□

E The proof of Theorem 2

Proof. From Theorem 1 in Imakura et al. (2021), if

$$\mathcal{S}_1 = \dots = \mathcal{S}_c \text{ and } \boldsymbol{\mu}_1 = \dots = \boldsymbol{\mu}_c \text{ and } \text{rank}(X^{\text{anc}} \bar{F}_k) = \tilde{m},$$

then we have

$$\tilde{X} = W \bar{F}_1 G_1 = \dots = W \bar{F}_c G_c,$$

where $W = [\mathbf{1}, X - \mathbf{1} \boldsymbol{\mu}_1^\top]$. Denote \mathbf{w}_i^\top as the i th row of W . Here, consider

$$t(\boldsymbol{\beta}') = [[1, \mu_1^1, \dots, \mu_1^m] \boldsymbol{\beta}', \beta'^1, \dots, \beta'^m]^\top \in \mathbb{R}^{m+1}.$$

then, we can express $\boldsymbol{\gamma}_{\text{CA}} = t(\boldsymbol{\beta}_{\text{CA}})$. Since $[1, \mathbf{x}_i^\top] \boldsymbol{\beta}' = \mathbf{w}_i^\top t(\boldsymbol{\beta}')$,

$$\begin{aligned}
\boldsymbol{\beta}_{\text{CA}} &= \arg \min_{\boldsymbol{\beta}' \in \mathbb{R}^{m+1}} \sum_i (\hat{\zeta}_i - \hat{\eta}_i [1, \mathbf{x}_i^\top] \boldsymbol{\beta}')^2 \\
&= \arg \min_{\boldsymbol{\beta}' \in \mathbb{R}^{m+1}} \sum_i (\hat{\zeta}_i - \hat{\eta}_i \mathbf{w}_i^\top t(\boldsymbol{\beta}'))^2.
\end{aligned}$$

Thus, γ_{CA} is equal to the solution of the following least squares problem:

$$\gamma_{\text{CA}} = \arg \min_{\gamma' \in \mathbb{R}^{m+1}} \sum_i (\hat{\zeta}_i - \hat{\eta}_i \mathbf{w}_i^\top \gamma')^2.$$

From the assumption $\gamma_{\text{CA}} \in \mathcal{S}_k$,

$$\begin{aligned} \gamma_k &= \bar{F}_k G_k \check{\gamma} \\ &= \arg \min_{\bar{F}_k G_k \gamma' \in \mathcal{S}_k} \sum_i (\hat{\zeta}_i - \hat{\eta}_i \mathbf{w}_i^\top \bar{F}_k G_k \gamma')^2 \\ &= \arg \min_{\gamma' \in \mathcal{S}_k} \sum_i (\hat{\zeta}_i - \hat{\eta}_i \mathbf{w}_i^\top \gamma')^2 \\ &= \gamma_{\text{CA}}. \end{aligned}$$

We used the assumptions $q_{\text{CA}}(\mathbf{x}_i) = \check{q}(\check{\mathbf{x}}_i)$ and $h_{\text{CA}}(\mathbf{x}_i) = \check{h}(\check{\mathbf{x}}_i)$ to transform the equation from line 2 to 3. It is obvious that β_{CA} and β_k are equal in all but the first element.

However,

$$\begin{aligned} \alpha_k &= [1, -\mu_k^1, \dots, -\mu_k^m] \gamma_k \\ &= [1, -\mu_1^1, \dots, -\mu_1^m] \gamma_{\text{CA}} \\ &= \alpha_{\text{CA}} \end{aligned}$$

where α_{CA} is the first element of β_{CA} . Then, $\beta_{\text{CA}} = \beta_k$. □

F Hyperparameters for candidate methods

Most hyperparameters of candidate methods for q and h are default parameters in scikit-learn (V1.2.2) and LightGBM (V3.3.5). The hyperparameters for q estimation are as follows.

LinearRegression (scikit-learn) fit_intercept: True, positive: False

RandomForestRegressor (scikit-learn) bootstrap: True, ccp_alpha: 0.0, criterion: squared_error, max_depth: None, max_features: 1.0, max_leaf_nodes: None, max_samples: None,

min_impurity_decrease: 0.0, min_samples_leaf: 1, min_samples_split: 2, min_weight_fraction_leaf: 0.0, n_estimators: 100, oob_score: False, warm_start: False

KNeighborsRegressor (scikit-learn) algorithm: auto, leaf_size: 30, metric: minkowski, metric_params: None, n_neighbors: 5, p: 2, weights: uniform

LGBMRegressor (LightGBM) boosting_type: gbdt, class_weight: None, colsample_bytree: 1.0, importance_type: split, learning_rate: 0.1, max_depth: -1, min_child_samples: 20, min_child_weight: 0.001, min_split_gain: 0.0, n_estimators: 100, num_leaves: 31, objective: None, reg_alpha: 0.0, reg_lambda: 0.0, subsample: 1.0, subsample_for_bin: 200000, subsample_freq: 0

SVR (scikit-learn) C: 1.0, cache_size: 200, coef0: 0.0, degree: 3, epsilon: 0.1, gamma: scale, kernel: rbf, max_iter: -1, shrinking: True, tol: 0.001

The hyperparameters for h estimation are as follows.

LogisticRegression (scikit-learn) C: 1.0, class_weight: None, dual: False, fit_intercept: False, intercept_scaling: 1, l1_ratio: None, max_iter: 100, multi_class: auto, n_jobs: None, penalty: none, solver: lbfgs, tol: 0.0001, warm_start: False

RandomForestClassifier (scikit-learn) bootstrap: True, ccp_alpha: 0.0, class_weight: None, criterion: gini, max_depth: None, max_features: sqrt, max_leaf_nodes: None, max_samples: None, min_impurity_decrease: 0.0, min_samples_leaf: 1, min_samples_split: 2, min_weight_fraction_leaf: 0.0, n_estimators: 100, oob_score: False, warm_start: False

KNeighborsClassifier (scikit-learn) algorithm: auto, leaf_size: 30, metric: minkowski, metric_params: None, n_neighbors: 5, p: 2, weights: uniform

LGBMClassifier (LightGBM) boosting_type: gbdt, class_weight: None, colsample_bytree: 1.0, importance_type: split, learning_rate: 0.1, max_depth: -1, min_child_samples: 20,

min_child_weight: 0.001, min_split_gain: 0.0, n_estimators: 100, num_leaves: 31, objective: None, reg_alpha: 0.0, reg_lambda: 0.0, subsample: 1.0, subsample_for_bin: 200000, subsample_freq: 0

SVC (scikit-learn) C: 1.0, break_ties: False, cache_size: 200, class_weight: None, coef0: 0.0, decision_function_shape: ovr, degree: 3, gamma: scale, kernel: rbf, max_iter: -1, probability: True, shrinking: True, tol: 0.001

G The results of the preliminary simulations

In the preliminary simulations, RMSE was calculated for the estimation of q and Brier score for the estimation of h using a two folds cross-validation with raw data. Table 5 shows the averages of 50 trials.

H Settings for the existing methods

To conduct the existing method, we used EconML (V0.14.1) and FedCI (<https://github.com/vothanhvinh/FedCI>). All hyperparameters of GRF (CausalForest) and FedCI are default values as follows.

CausalForest (EconML) criterion: mse, fit_intercept: True, honest: True, inference: True, max_depth: None, max_features: auto, max_samples: 0.45, min_balancedness_tol: 0.45, min_impurity_decrease: 0.0, min_samples_leaf: 5, min_samples_split: 10, min_var_fraction_leaf: None, min_var_leaf_on_val: False, min_weight_fraction_leaf: 0.0, n_estimators: 100, subforest_size: 4, warm_start: False

FedCI n_iterations:2000, learning_rate:1e-3

For X-Learner, candidate methods for estimation of the outcome and propensity score have the hyperparameters described in supplemental material F. For SR, we considered the

regression model to consist of a constant term and a cross term between the covariates and the treatment as

$$y_i = \text{const.} + z_i(\beta^0 + x_i^1\beta^1 + \dots + x_i^m\beta^m) + \varepsilon_i.$$

I The all results of Simulation III

Figures 4, 6, 7 and 8 represent the results of Simulation III for the financial assets dataset. In the RMSE of coefficients and the consistency rate of significance of coefficients shown in Figures 7 and 8, DC-DML results for party1 using LPP are worse than for IA-DML in some cases. However, in most other cases shown in Figures 4, 6, 7 and 8, DC-DML results are better than IA-DML. In addition, the dimensionality reduction method combined with bootstrapping shows robust results. No SR results are better than IA-DML.

Figures 5, 9, 10 and 11 represent the results of Simulation III for the jobs dataset. DC-DML results are worse than IA-DML when using LPP for the consistency rate of significance of CATE, and using LPP, LPP+B or FA+B for the consistency rate of significance of coefficients. However, DC-DML results are often better than IA-DML. DC-DML performs better than IA-DML particularly in the RMSEs of CATE and coefficients in most cases. Moreover, as with the financial assets dataset, the dimensionality reduction method combined with bootstrapping shows robust results. SR results are often worse than IA-DML.

On both datasets, there were cases where better performance was not achieved with DC-DML using LPP, especially. This suggests that the choice of dimensionality reduction method has a significant impact on the performance of DC-DML.

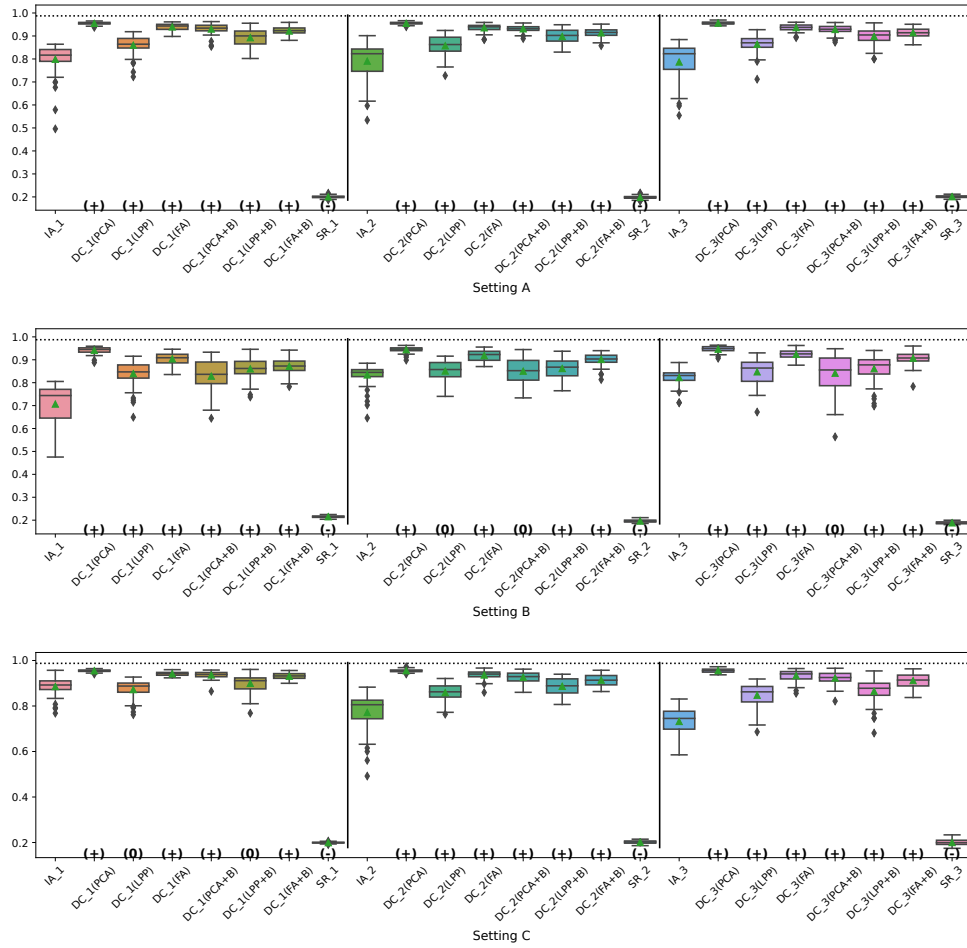


Figure 6: The consistency rate of significance of CATE in Simulation III for the financial assets dataset.

Algorithm 1 Data collaboration quasi-experiment (DC-QE)

Input: covariates X , treatments Z , outcomes Y .

Output: estimated treatment effect $\hat{\tau}$.

user-k-side

- 1: Generate anchor dataset X_k^{anc} and share it with all users.
 - 2: Set X^{anc} .
 - 3: Generate f_k .
 - 4: Compute $\tilde{X}_k = f_k(X_k)$.
 - 5: Compute $\tilde{X}_k^{\text{anc}} = f_k(X_k^{\text{anc}})$.
 - 6: Share \tilde{X}_k , \tilde{X}_k^{anc} , Z_k and Y_k to the analyst.
-

analyst-side

- 7: Get \tilde{X}_k , \tilde{X}_k^{anc} , Z_k and Y_k for all k .
 - 8: Set \tilde{X}_k and \tilde{X}_k^{anc} .
 - 9: Compute g_k from \tilde{X}_k^{anc} for all k such that $g_k(\tilde{X}_k^{\text{anc}}) \approx g_{k'}(\tilde{X}_{k'}^{\text{anc}})$ ($k \neq k'$).
 - 10: Compute $\check{X}_k = g_k(\tilde{X}_k)$ for all k .
 - 11: Set \check{X} , Z and Y .
 - 12: Estimate propensity scores $\hat{\alpha}$ from \check{X} and Z .
 - 13: Estimate average treatment effect $\hat{\tau}$ from $\hat{\alpha}$ and Y using existing ways (matching, weighting and so on).
-

Algorithm 2 Data collaboration double machine learning (DC-DML)

Input: covariates X , treatments Z , outcomes Y .

Output: β_k , $\text{Var}(\gamma_k)$ and $\text{Var}(\alpha_k)$.

user- k -side

- 1: Generate anchor dataset X_k^{anc} and share it with all users.
 - 2: Set X^{anc} .
 - 3: Generate F_k and μ_k .
 - 4: Compute $\tilde{X}_k = (X_k - \mathbf{1}\mu_k^\top)F_k$.
 - 5: Compute $\tilde{X}_k^{\text{anc}} = (X_k^{\text{anc}} - \mathbf{1}\mu_k^\top)F_k$.
 - 6: Share $[\mathbf{1}, \tilde{X}_k]$, $[\mathbf{1}, \tilde{X}_k^{\text{anc}}]$, Z_k and Y_k to the analyst.
-

analyst-side

- 7: Get $[\mathbf{1}, \tilde{X}_k]$, $[\mathbf{1}, \tilde{X}_k^{\text{anc}}]$, Z_k and Y_k for all k .
 - 8: Set $[\mathbf{1}, \tilde{X}_k]$ and $[\mathbf{1}, \tilde{X}_k^{\text{anc}}]$.
 - 9: Compute G_k from \tilde{X}_k^{anc} for all k such that $[\mathbf{1}, \tilde{X}_k^{\text{anc}}]G_k \approx [\mathbf{1}, \tilde{X}_{k'}^{\text{anc}}]G_{k'}$ ($k \neq k'$).
 - 10: Compute $\check{X}_k = [\mathbf{1}, \tilde{X}_k]G_k$ for all k .
 - 11: Set \check{X} , Z and Y .
 - 12: Compute function \check{q} and \check{h} using \check{X} , Z and Y .
 - 13: Compute residuals $\hat{\eta}$ and $\hat{\zeta}$ using \check{q} , \check{h} , \check{X} , Z and Y .
 - 14: Obtain $\check{\gamma}$ and $\text{Var}(\check{\gamma})$ as the least square solution of (4.1.2).
 - 15: Return $R_k^{\text{Point}} = G_k\check{\gamma}$ and $R_k^{\text{Var}} = G_k\text{Var}(\check{\gamma})G_k^\top$ to all user k .
-

user- k -side

- 16: Set R_k^{Point} and R_k^{Var} .
 - 17: Compute β_k , $\text{Var}(\gamma_k)$ and $\text{Var}(\alpha_k)$.
-

Algorithm 3 A bootstrap-based dimensionality reduction for DC-DML

Input: covariates X_k , treatments Z_k , outcomes Y_k .

Output: F_k .

- 1: **for** $b = 1, \dots, \tilde{m}_k$: **do**
 - 2: Set X_k^b , Z_k^b and Y_k^b by a random sampling of size pn_k from X_k , Z_k and Y_k .
 - 3: Compute γ_b from X_k^b , Z_k^b and Y_k^b by the DML procedure.
 - 4: **end for**
 - 5: Return $F_k = [\tilde{\gamma}_1, \dots, \tilde{\gamma}_{\tilde{m}_k}]$.
-

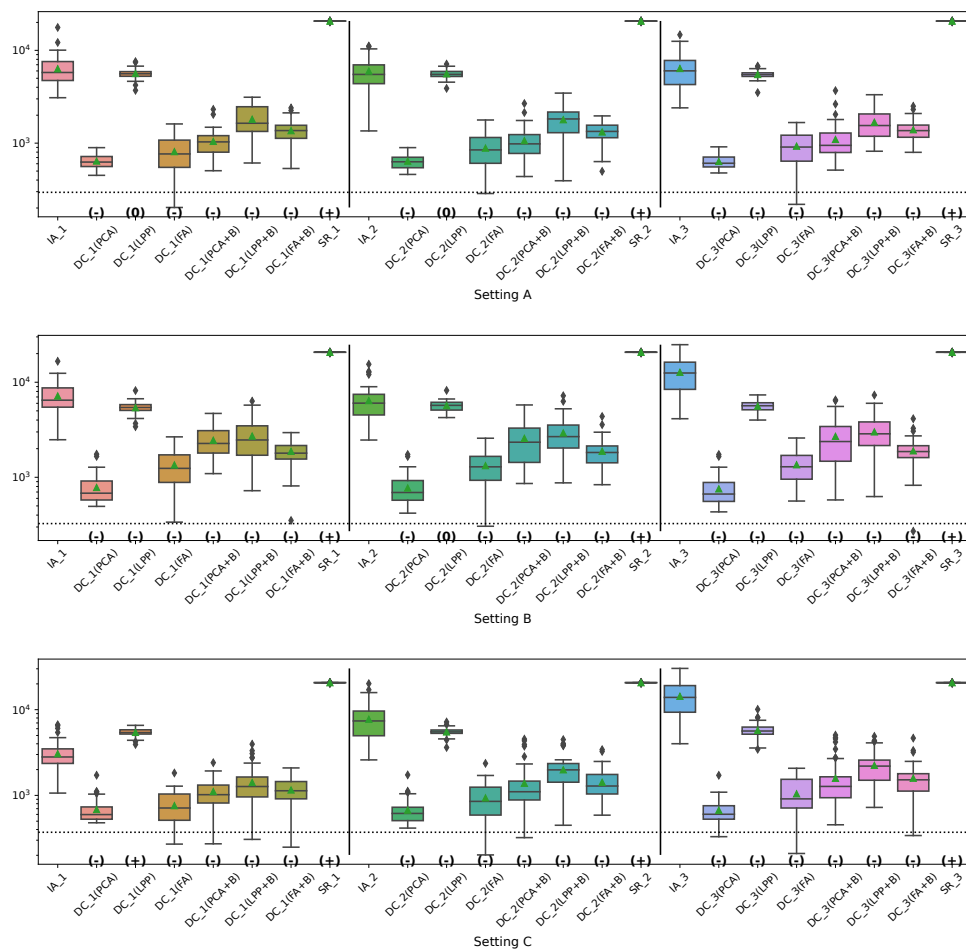


Figure 7: The RMSE of coefficients in Simulation III for the financial assets dataset.

Simulation II			
q	RMSE	h	Brier score
Multiple regression	2.5613	Logistic regression	0.2579
Random forests	2.5308	Random forests	0.1532
K-nearest neighbor	2.8690	K-nearest neighbor	0.1665
LGBM	2.5734	LGBM	0.1733
SVM	2.2333	SVM	0.1488

Simulation III for the financial assets dataset			
q	RMSE	h	Brier score
Multiple regression	55827.4190	Logistic regression	0.2014
Random forests	58048.7840	Random forests	0.2151
K-nearest neighbor	57861.6099	K-nearest neighbor	0.2339
LGBM	56665.7031	LGBM	0.2047
SVM	65450.8516	SVM	0.2080

Simulation III for the jobs dataset			
q	RMSE	h	Brier score
Multiple regression	10963.5250	Logistic regression	0.1699
Random forests	12058.0681	Random forests	0.1628
K-nearest neighbor	11981.2699	K-nearest neighbor	0.1751
LGBM	11503.7386	LGBM	0.1719
SVM	15613.6765	SVM	0.1912

Table 5: The results of the preliminary simulations.

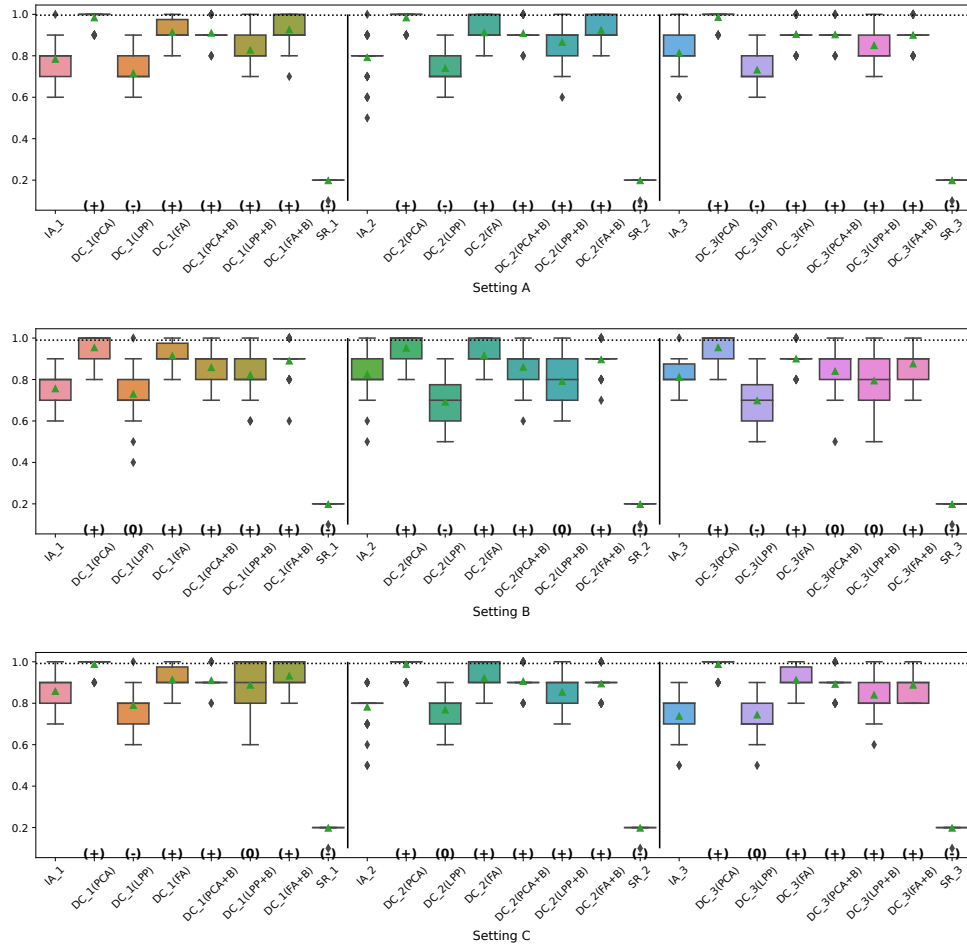


Figure 8: The consistency rate of significance of coefficients in Simulation III for the financial assets dataset.

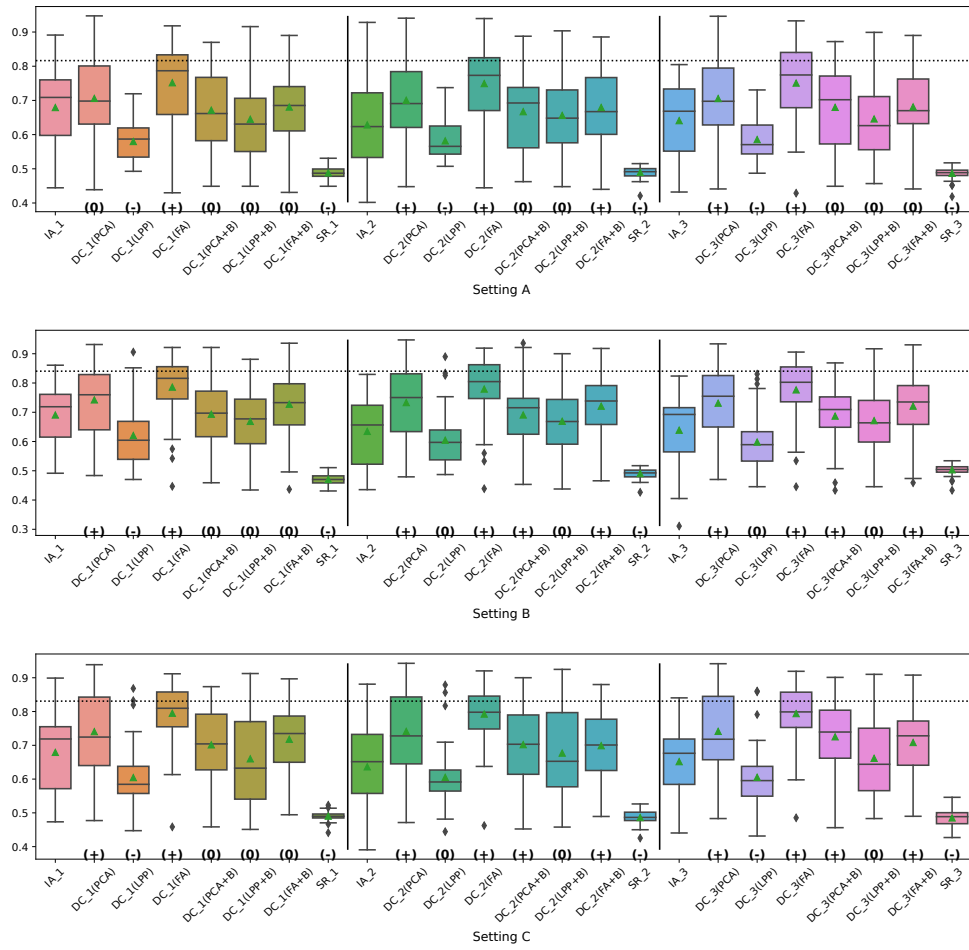


Figure 9: The consistency rate of significance of CATE in Simulation III for the jobs dataset.

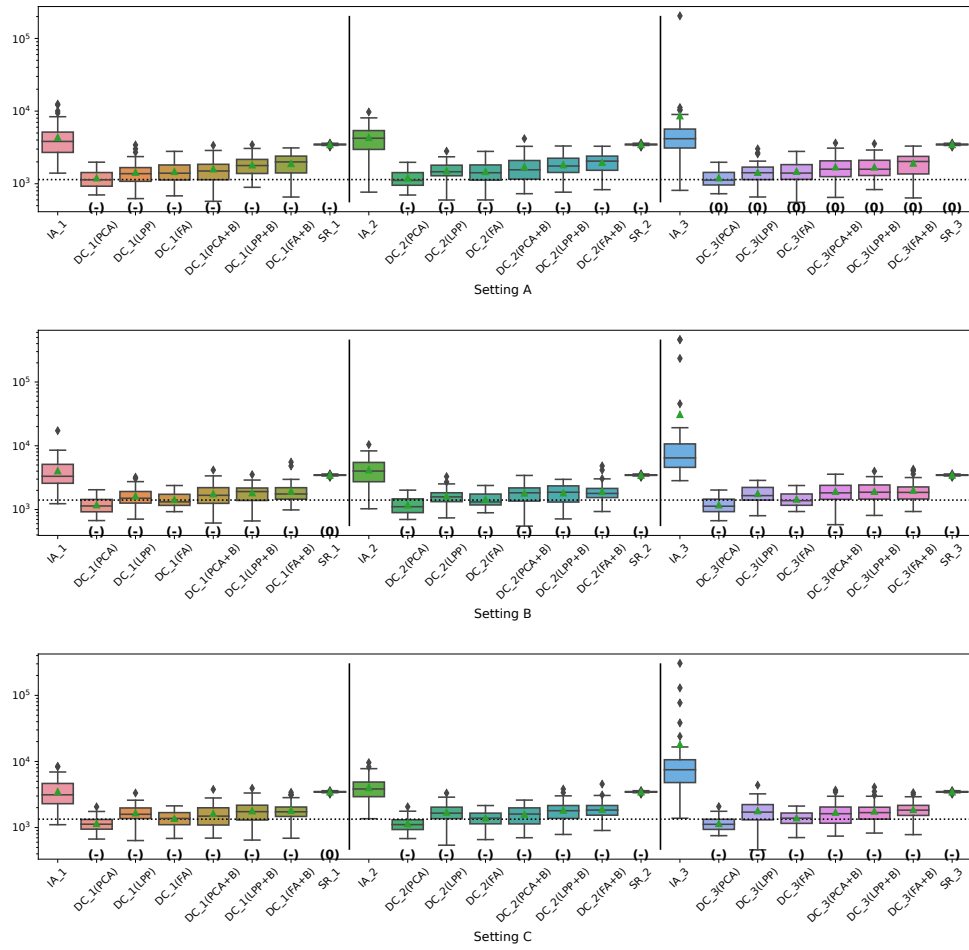


Figure 10: The RMSE of coefficients in Simulation III for the jobs dataset.

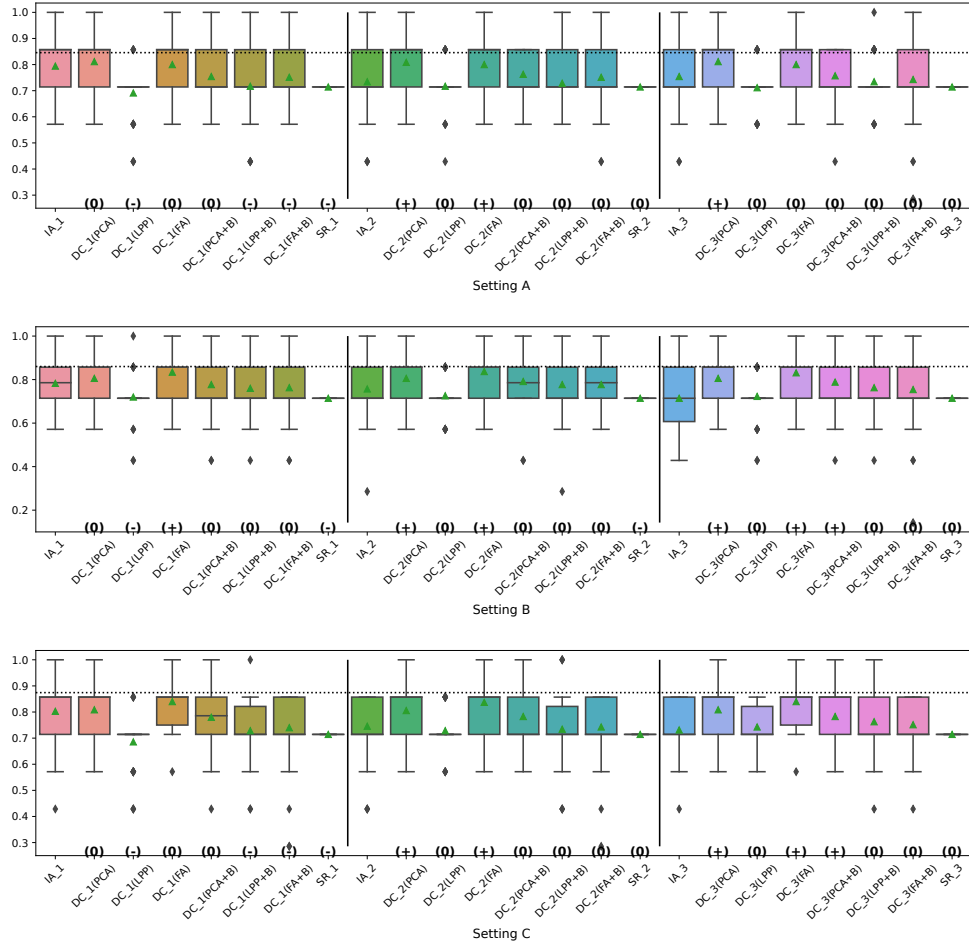


Figure 11: The consistency rate of significance of coefficients in Simulation III for the jobs dataset.